Karlsruhe Institute of Technology

Institut für Theoretische Physik

Anomalous Couplings within Standard Model Effective Field Theory in $t\bar{t}H$ Production at NLO QCD

Master's Thesis of

Marijn van Geest

at the Department of Physics
Institute for Theoretical Physics (ITP)

Reviewer:	Prof. Dr. Gudrun Heinrich
Second reviewer:	PD Dr. Stefan Gieseke
Advisor:	Dr. Marius Höfer

November 8, 2023 – October 30, 2024

I declare that I have developed and written the enclosed thesis completely by myself, and have not used sources or means without declaration in the text.

Karlsruhe; October 30, 2024

. . . . . .

(Marijn van Geest)

Abstract

This thesis deals with the implementation of Standard Model Effective Field Theory (SMEFT) in the WHIZARD + GOSAM framework, two programs that are designed to set up matrix elements in the context of quantum field theories and to numerically evaluate the associated cross sections. The process $pp \to t\bar{t}H$ serves as the main orientation for this implementation and is also used for validation. First, there is a summary of the most important theory segments of the Standard Model and effective field theories, which will be used throughout this thesis. Subsequently, the various practical steps that are important in this implementation as well as the special care and complications involved are presented and discussed. One of the main topics is the specific construction of the physics model used for the implementation, which includes, for example, the required counterterms and general renormalization. A possible generalization in dealing with the SMEFT Warsaw basis is also discussed throughout. The model is then embedded in the framework using the UFO format. At the end, numerical values are presented with the described procedure, whereby a validation of the procedure is carried out by means of reference values.

Zusammenfassung

Die vorliegende Arbeit beschäftigt sich mit der Implementierung von Standard Model Effective Field Theory (SMEFT) in die Kombination Whizard + GoSam, zwei Programme die darauf ausgelegt sind Matrixelemente im Rahmen von Quantenfeldtheorien aufzustellen und die zugehörigen Wirkungsquerschnitte numerisch auszuwerten. Dabei dient der Prozess $pp \to t\bar{t}H$ als zentrale Orientierung für diese Implementierung. Zunächst sind die wichtigsten Ausschnitte aus der Theorie zu dem Standardmodell sowie zu effektiven Feldtheorien zusammengefasst, welche durchgehend in der Arbeit verwendet werden. Im Anschluss werden die verschiedenen Schritte, welche bei dieser Umsetzung wichtig sind, sowie die speziellen Sorgfältigkeiten und Komplikationen, die damit einher gehen, dargestellt und diskutiert. Das Hauptthema ist dabei die spezifische Konstruktion des für die Implementierung verwendeten Physikmodells, worunter beispielsweise die benötigten Counterterme und generelle Renormierung fallen. Eine mögliche Verallgemeinerung im Umgang mit der SMEFT Warsaw-Basis wird hier ebenfalls durchgehend verwendet. Das Modell wird dann mit dem UFO-Format in den Programmablauf eingebetet. Am Ende werden einige numerische Werte mit dem dargestellten Vorgehen präsentiert, wobei eine Validierung des Verfahrens anhand von Vergleichswerten vorgenommen wird.

Contents

List of Figures

List of Tables

1. Introduction

1.1. Motivation

The Standard Model of particle physics has been a very successful theory, correctly predicting experimental findings with high accuracy. However, despite its success, there are some inconsistencies with other observations leading to the reasonable conclusion that it must be incomplete. One example would be the ongoing failure of the Standard Model to provide a suitable particle candidate to explain dark matter. The absence of interactions that yield possible interpretations to the baryon asymmetry in the universe is another shortcoming. This is why multiple approaches are studied in order to extend the Standard Model with yet unknown new physics.

After being theoretically predicted [1–6], the Higgs boson has been the most recent addition to the Standard Model and was discovered in 2012 at the CERN LHC Run I program [7, 8]. Due to its recent discovery, it seems natural to examine this object more closely. Its coupling to fermions is proportional to their mass, which is why Higgs production in association with a top quark is an intriguing process to study since this quark is particularly heavy, sitting at around $173\,\mathrm{GeV}$. In practice, the process $pp \to t\bar{t}H$ is the most prominent when it comes to probing this coupling at hadron colliders. It was first observed in 2018 by the CMS and ATLAS collaborations at CERN in 2018 [9, 10], providing a first experimental point of contact to this potential window to new physics.

While some popular SM extension attempts like supersymmetry [11] or the inclusion of Axions [12] choose to construct a specific model, there also exists a model-independent way of theoretically describing possible new physics effects at higher energy scales. The latter is mostly realized through effective field theories [13, 14], where the Standard Model is mathematically extended with an approximation series based on a generic energy scale where one would expect new physics to take place. The Standard Model then becomes a low energy approximation in regards to this scale, which is often chosen to be at $1\,\mathrm{TeV}$. This would therefore explain the apparent absence of anomalous findings by its suppression due to the energies that are typically reached at interactions in colliders. The process $pp \to t\bar{t}H$ has also already been investigated in several studies with regard to anomalous effects like CP-violations and effective operators [15–18], mainly by means of computer-aided numerical simulations. Of course, it is just as important to analyze the experimental data in this sector [19]. In the case of effective field theories, this can lead to numerous important constraints of their parameters [20]. In order to confirm anomalous findings experimentally, it remains crucial to improve theoretical predictions and develop the necessary tools to correctly identify the effects and magnitude of potential anomalous physics.

1.2. The Standard Model of Particle Physics

The Standard Model (SM) is the mathematical framework and collection of all known particles (see figure 1.1), their properties and interactions. Usually it is formulated as a Lagrangian (a Lagrange density) in the context of a quantum field theory, which can be written as

$$\mathcal{L}_{\mathrm{SM}} = \mathcal{L}_{QCD} + \mathcal{L}_{\mathrm{EW}} + \mathcal{L}_{\mathrm{H}} + \mathcal{L}_{\mathrm{Yukawa}} + \mathcal{L}_{Gauge-Fixing} + \mathcal{L}_{\mathrm{Ghost}} \,.$$

The different contributions as well as the important effects of spontaneous symmetry breaking (SSB) are briefly summarized in the following subsections.

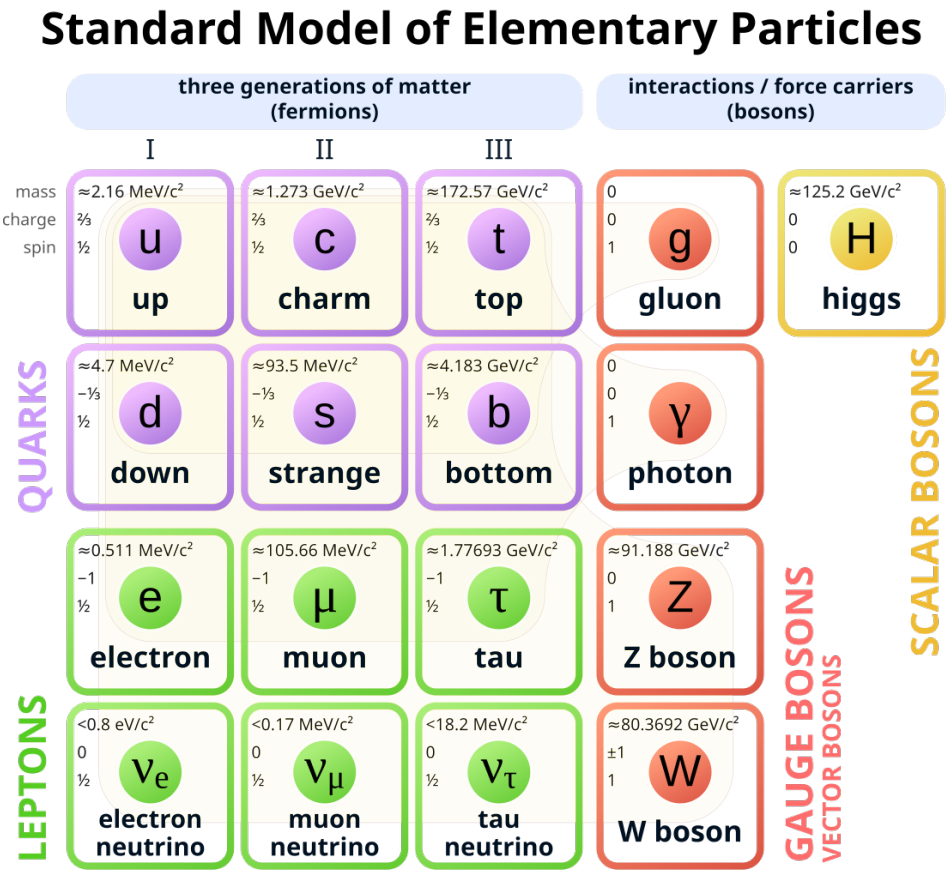

Figure 1.1.: Particle content of the Standard Model. Given with their approximate masses, charge and spin quantum numbers. As of 2024. Taken from [21]

1.2.1. Quantum Chromodynamics $\mathcal{L}_{QCD}$

In the QCD part of the SM Lagrangian, the kinetic term of the gluon fields is present together with the interaction terms between quarks and gluons, forming the main formalism in order to explain the strong nuclear force. It is implemented as a Yang-Mills gauge theory of an $\mathrm{SU}(3)$ symmetry group, representing the colour quantum number. It is written as

$$\mathcal{L}_{QCD} = i \sum_j \overline{\psi}_j \, \gamma^\mu D_\mu \, \psi_j - \frac{1}{4} G^a_{\mu\nu} G^{a\,\mu\nu} \ ,$$

where the ψ are Dirac spinors representing the different quark fields, while the sum iterates over all different flavours. The covariant derivative from this equation is defined as

$$D_\mu = \partial_\mu + i g_s T^a G^a_\mu \ .$$

Here, the T^a are the generators of $\mathrm{SU}(3)$, which are sometimes also written as $T^a = \lambda^a/2$, where λ^a are the Gell-Mann matrices. The G^a_μ are the gluon gauge fields with their colour index a. This first term therefore produces the kinetic quark terms as well as interactions between quarks and gluons. The kinetic gluon term contains the gluon field strength tensor, which is defined as

$$G^a_{\mu\nu} = \partial_\mu G^a_\nu - \partial_\nu G^a_\mu - g_s f^{abc} G^b_\mu G^c_\nu \ .$$

Therefore, this expression in the Lagrangian also produces terms that represent self-interactions of the gluon. The occurring f^{abc} are the structure constants of the gauge group and satisfy the commutation relation

$$[T^a, T^b] = i f^{abc} \, T^c \ .$$

The construction of this Lagrangian ensures that it is invariant under local $\mathrm{SU}(3)$ gauge transformations.

1.2.2. Electroweak Sector $\mathcal{L}_{EW}$

The electroweak sector implements the interactions based on the weak isospin and hypercharge quantum numbers that are represented by three $\mathrm{SU}(2)$ gauge fields W^a_μ and the $\mathrm{U}(1)$ gauge field B_μ respectively. Its Lagrangian can be written as

$$\mathcal{L}_{EW} = i \sum_{\psi,\,j} \overline{\psi}_{\mathrm{L},j} \gamma^\mu D_{\mathrm{L}\,\mu} \, \psi_{\mathrm{L},j} + i \sum_{\psi,\,j} \overline{\psi}_{\mathrm{R},j} \gamma^\mu D_{\mathrm{R}\,\mu} \, \psi_{\mathrm{R},j} - \frac{1}{4} W^a_{\mu\nu} W^{a\,\mu\nu} - \frac{1}{4} B_{\mu\nu} B^{\mu\nu} \ .$$

The fermionic part is seperated into a left-handed (doublet) and right-handed (singlet) part. Due to observations in nature, the weak interaction has shown to only act upon left-handed particles, which is why this distinction is necessary. The sum over ψ iterates through the up- and down-type quarks as well as the leptons, while the sum over j goes though the three generations of fermions. Note that the neutrinos are not included in the the right-handed part, since all observed neutrinos are left-handed (and all anti-neutrinos right-handed).

The covariant derivatives then become

$$D_{\mathrm{L}\,\mu} = \partial_\mu + i\frac{g'}{2} Y\, B_\mu + i\frac{g}{2} I^a\, W_\mu^a$$
$$D_{\mathrm{R}\,\mu} = \partial_\mu + i\frac{g'}{2} Y\, B_\mu\,.$$

Y is the (weak) hypercharge, while the I^a are the components of the weak isospin, which are represented by the Pauli matrices. One has to note here that the different covariant kinetic terms in $\mathcal{L}_{\mathrm{EW}}$ and $\mathcal{L}_{QCD}$ for the fermions are written in such a way that the distinction between the QCD and EW contributions becomes clearer, but each fermion receives only one "pure" kinetic term of the form $\partial_\mu\psi\partial^\mu\psi$ in total.

In analogy to QCD, the electroweak sector is invariant under local $\mathrm{SU}(2)\times\mathrm{U}(1)$ transformations. This sector is significantly changed after the spontaneous symmetry breaking in the form of the Higgs mechanism. This is discussed further in the corresponding section 1.2.3 as well as section 1.2.4

1.2.3. Higgs Sector $\mathcal{L}_{\mathrm{H}}$ and the Higgs Mechanism

Up to now, the gauge bosons as well as the fermions would not have dedicated mass terms, although experiments have shown a clear evidence of masses. In fact, canonical mass terms would break the gauge invariance, which is an important property of the SM. The Higgs mechanism was proposed to solve this issue [1–6]. The Higgs field is a scalar field defined as a complex doublet out of the $\mathrm{SU}(2)$ group

$$\varphi = \begin{pmatrix} \varphi^+ \\ \varphi^0 \end{pmatrix}\,,$$

where the Lagrnagian given to this field is

$$\mathcal{L}_{\mathrm{H}} = (D_\mu\,\varphi)^\dagger (D^\mu\,\varphi) + \mu^2\,\varphi^\dagger\varphi - \lambda(\varphi^\dagger\varphi)^2\,,$$

where μ and λ are generic parameters to shape its potential. One must require $\mu^2 > 0$ and $\lambda > 0$, so that the potential has the right shape in order for the mechanism to work. It is also constructed to respect the $\mathrm{SU}(2)\times\mathrm{U}(1)$ symmetry.

The covariant derivative is the same as for the left-handed particles in the electroweak sector. By minimizing the potential and applying a suitable gauge transformation (unitary gauge), one can show that the expectation value of the Higgs field around its ground state becomes

$$\langle\varphi\rangle = \frac{1}{\sqrt{2}}\begin{pmatrix} 0 \\ v+h \end{pmatrix}\,,$$

where v is the constant vacuum expectation value at $v \approx 246\,\mathrm{GeV}$ and h is the Higgs boson. This is still invariant under $\mathrm{U}(1)$ transformations. The main idea is that this spontaneous symmetry breaking takes place and the Higgs field can be expressed around its ground state.

From the kinetic term in the Lagrangian then follows a kinetic term for the Higgs boson but also mass terms for the fields

$$\frac{1}{\sqrt{2}}(W_\mu^1 \pm iW_\mu^2) := W_\mu^\mp$$
$$g\,W_\mu^3 - g'B_\mu := \sqrt{g^2+g'^2}\,Z_\mu\ ,$$

which then define the charged vector bosons $W^\pm$ and the Z^0 boson associated with the weak interaction. These field combinations emerge from the contraction of the field components with the structures in the covariant derivative, so they will also naturally appear throughout the electroweak Lagrangian. In addition, the combination

$$g\,W_\mu^3 + g'B_\mu := \sqrt{g^2+g'^2}\,A_\mu\ ,$$

does also appear which one then needs to define as another field: The photon. This is generally formulated in a mixing matrix

$$\begin{pmatrix} A \\ Z \end{pmatrix} = \begin{pmatrix} \cos(\theta_w) & \sin(\theta_w) \\ -\sin(\theta_w) & \cos(\theta_w) \end{pmatrix} \begin{pmatrix} B \\ W^3 \end{pmatrix}\ ,$$

where the θ_w is the weak mixing angle. The Higgs mechanism therefore introduces the mass of the bosons of the weak interaction, while the photon remains massless. The resulting electromagnetic theory preserves the $\mathrm{U}(1)$ symmetry, which is why this process is often described as the breaking of the electroweak symmetry to the combined electromagnetic symmetry $\mathrm{SU}(2)_w \times \mathrm{U}(1)_Y \to \mathrm{U}(1)_{\mathrm{EM}}$.

1.2.4. Yukawa Sector $\mathcal{L}_{\mathrm{Yukawa}}$ and Quark Mixing

The gauge invariance of the fermionic mass terms can also be correctly implemented by the Higgs mechanism by introducing Yukawa interactions between the Higgs boson and the fermions. It is necessary, since a naive fermionic mass term would look like

$$-m_j \cdot \overline{\psi}_j\psi_j = -m_j \cdot \left(\overline{\psi}_{j,\mathrm{L}}\psi_{j,\mathrm{R}} + \overline{\psi}_{j,\mathrm{R}}\psi_{j,\mathrm{L}}\right)\ ,$$

which is a consequence of the fact, that unity can be expressed in terms of the projection operators for the different chirality components ($\mathbb{1} = P_\mathrm{L} + P_\mathrm{R}$).

Since the left-handed doublets transform differently under a gauge transformation as the right-handed singlets, a term like this would break gauge invariance. However, by including the Higgs field in a Yukawa coupling together with the fermions restores this gauge invariance, since φ is an $\mathrm{SU}(2)$ doublet itself and the gauge transformations are unitary. The only thing one needs to consider is the conservation of hypercharge, which is why the up-type quarks need an insertion of the charge conjugate version of the Higgs field, which will be denoted as $\widetilde{\varphi}$. The total Yukawa Lagrangian is then typically written as

$$\mathcal{L}_{\mathrm{Yukawa}} = (Y_u)_{ij}(\overline{Q}_\mathrm{L})_i\,\widetilde{\varphi}\,(u_\mathrm{R})_j + (Y_d)_{ij}(\overline{Q}_\mathrm{L})_i\,\varphi\,(d_\mathrm{R})_j + (Y_e)_{ij}(\bar{l}_\mathrm{L})_i\,\varphi\,(e_\mathrm{R})_j + \text{h.c.}\ .$$

Here, the field Q_{L} represents the left-handed quark doublet, whereas l_{L} is the left-handed lepton doublet. The u_{R}, d_{R} and e_{R} are the right-handed up-type quark, down-type quark and electron-type lepton fields respectively. The Y_j are the Yukawa matrices.

A term like this then behaves like

$$(Y_d)_{ij}(\overline{Q}_{\mathrm{L}})_i\,\varphi\,(d_{\mathrm{R}})_j + \text{h.c.} \quad \xrightarrow{\text{SSB}} \quad (Y_d)_{ij}\left(\frac{v+h}{\sqrt{2}}\right)\left[(\overline{Q}_{\mathrm{L}})_i\,(d_{\mathrm{R}})_j + (\overline{d}_{\mathrm{R}})_j\,(Q_{\mathrm{L}})_i\right] \ ,$$

which after the spontaneous symmetry breaking introduces the possibility for mass terms of fermions as the part proportional to v as well as the interaction term between the fermions and the Higgs boson as the part proportional to h. Although a matrix structure like this is required, since the different fermion generations can generally mix with eachother, one can choose a unitary transformation in order to diagonalize these Yukawa matrices, so that each flavour obtains their clear individual mass term. The masses are then given by

$$m_j = \frac{y_j \cdot v}{\sqrt{2}} \quad \Rightarrow \quad y_j = \sqrt{2}\,\frac{m_j}{v} \ ,$$

with the resulting Yukawa coupling y_j for flavour j. It also follows that the coupling constant of the Higgs-fermion interaction, which is always proportional to the Yukawa coupling, is proportional to the fermion mass.

However, this transformation will introduce a matrix structure in the electroweak sector, which leads to different couplings based on flavour in the interaction between the fermions and the W and Z bosons. Therefore, it is said that the mass eigenstates and the flavour eigenstates of fermions are not equal in general. This matrix structure can be defined as acting only "to the right" and is known as the Cabibbo–Kobayashi–Maskawa (CKM) matrix in the context of quarks. It effectively quantifies the probability that a quark of one flavour transitions to a quark of another flavour during weak interactions.

1.2.5. Gauge-fixing and Ghost fields $\mathcal{L}_{\mathrm{G}auge-Fixing} + \mathcal{L}_{\mathrm{G}host}$

When constructing the Standard Model, gauge invariance and the resulting symmetries are very important. However, in general, these will also introduce redundancies and non-physical degrees of freedom. To remove these additional dependencies, one can use some gauge fixing procedure, which will ensure a unique description of the system. The unitary gauge is one possible choice which was touched upon in section 1.2.3. Another common choice is the Rξ gauge.

In general, specific terms are added to the Lagrangian to ensure the unique description that can be collected in $\mathcal{L}_{\mathrm{G}auge-Fixing}$. Doing so will result in additional terms to the Standard Model that can undermine unitarity (the property that correctly normalizes the theoretical predictions coming from it). Therefore, the final step is to add other auxiliary particles which repair unitarity. These are called Ghost particles or Faddeev-Popov Ghosts and are therefore contained in the $\mathcal{L}_{\mathrm{G}host}$ Lagrangian. The Ghost Lagrangian will depend on the gauge-fixing procedure used. In unitary gauge, there will be no $\mathcal{L}_{\mathrm{G}auge-Fixing}$ and therefore also no $\mathcal{L}_{\mathrm{G}host}$. A general discussion of both in the Rξ gauge can be found in [22].

1.3. (Standard Model) Effective Field Theory

In a quantum field theory, a physical model is described by its Lagrangian, which includes all the fields and their interactions relevant to the model. The interaction terms of the Lagrangian are a product of multiple fields and can be used to deduce the Feynman rules for these specific interactions, which quantify the probability that such a process in between a suitable initial state and final state occurs.

In general, the deduced Feynman rules are dependent on the energy scale of the interacting particles. When the probed scale is small enough, the momenta of external particles can often be neglected in comparison to the masses or momenta of more heavy intermediate particles of a certain process. This can lead to a simplified description of an interaction. A famous example is the Fermi interaction. By starting with the SM, the process $\mu^- \to \nu_\mu \bar{\nu}_e e^-$ symbolically receives the amplitude

$$\mathcal{A} \sim \bar{u}_e \left(g\Gamma^{\mu'} \right) v_{\nu_e} \left[\frac{1}{k^2 - M_W^2} \right] \bar{u}_{\nu_\mu} \left(g\Gamma_{\mu'} \right) u_\mu \ ,$$

where the expression in the $[\dots]$ parentheses comes from the W boson propagator with momentum k. By now assuming $k^2 \ll M_W^2$ one can write this amplitude as

$$\to \mathcal{A} \sim -\bar{u}_e \left(g\Gamma^{\mu'} \right) v_{\nu_e} \left[\frac{1}{M_W^2} + \frac{k^2}{M_W^4} + \mathcal{O}(\frac{k^4}{M_W^6}) \right] \bar{u}_{\nu_\mu} \left(g\Gamma_{\mu'} \right) u_\mu \ .$$

In this case the observed energy scale of the process is assumed to be less than the W boson mass. Through this approximation, the process at leading order looks like an interaction between four leptons with a coupling constant proportional to g^2/M_W^2 which is in turn proportional to Fermi's constant G_F. So the historically relevant Fermi interaction is an effective interaction for a low energy approximation of the Standard Model, where the W boson vanishes from the theory and the corresponding Feynman diagram is "pinched" at the propagator (see figure 1.2). In this case, after the approximation, the corresponding part in the Lagrangian of the theory can be written as

$$\mathcal{L}_{EFT} \supset \frac{C}{M_W^2} \left(\bar{\nu}_\mu \Gamma^{\mu'} \mu \right) \left(\bar{e}\, \Gamma_{\mu'} \nu_e \right) := \frac{C}{M_W^2} \mathcal{O}_F \ ,$$

where $\mathcal{O}_F$ can now be seen as an effective operator used to describe this new interaction. The dimenionless constant C in front is called the Wilson coefficient, with $C \sim g^2$ in this case. Motivating the effective operator based on the full theory is the top-down approach, however, one can also construct all possible operators that include the low-energy fields while also respecting the applicable symmetries and include them in the theory based on their dimension, which is the bottom-up way. Doing this for all possible processes in a given theory will result into an *Effective Field Theory* (EFT), containing generally multiple effective operators, describing direct interactions at the chosen energy scale, which would otherwise occur as a combination of multiple chained interactions connected by the more heavy particles.

Such a Lagrangian is integrated over 4-dimensional spacetime to produce the corresponding action. When working with natural units, the action has to be dimensionless since it can be seen as directly proportional to $\hbar$.

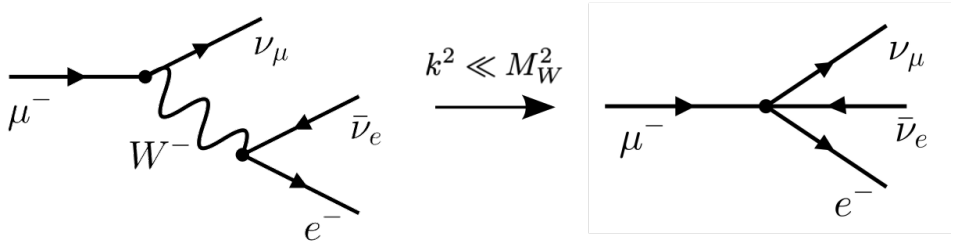

Figure 1.2.: The diagrammatic representation of the effect small momenta can have in an interaction. The approximation $k^2 \ll M_W^2$ leads to an effective four-fermion vertex. The Feynman diagrams were made with FeynGame [23].

The integration measure has a mass dimension of $[\mathrm{d}^4x]_m = -4$, which means that $[\mathcal{L}]_m = 4$. Therefore, each term in the Lagrangian needs a mass dimension of 4. This is achieved by combinations of the intrinsic mass dimension of each field and the (coupling) constants in each term. In general, an EFT-Lagrangian can be written as

$$\mathcal{L} = \mathcal{L}_0 + \sum_{\substack{i \\ d_i > 4}} \frac{C_i^{(d_i)}}{\Lambda^{d_i-4}} \mathcal{O}_i^{(d_i)} \,, \tag{1.1}$$

where $\mathcal{L}_0$ is the canonical Lagrangian of the theory containing only the fields with masses up to the energy scale of interest E. The effective operators $\mathcal{O}_i^{(d_i)}$ with mass dimension $d_i > 4$ only contain fields and couplings introduced in $\mathcal{L}_0$. For dimensional reasons, one needs to add a factor with mass dimension $-(d_i - 4)$, ensuring the correct dimension overall. This is done by dividing by Λ^{d_i-4}, where Λ is a parameter, representing the energy scale of the high energy theory with $[\Lambda]_m = 1$, and multiplying with $C_i^{(d_i)}$, the Wilson coefficients. This therefore takes the form of an approximation series in powers of $1/\Lambda$, whereby all effective operators are increasingly suppressed with increasing orders. With this formalism, a theory can effectively be described in a low energy approximation where the typical scale is $E \ll \Lambda$. All fields with a mass $m \gtrsim \Lambda$ will not occur in this theory explicitly. The operators $\mathcal{O}_i^{(d_i)}$ then generally consist of all combinations of all relevant fields, while also respecting the required symmetries and other restrictions of the model.

In the context of the Standard Model, where $\mathcal{L}_0 = \mathcal{L}_{SM}$, a bottom-up EFT approach can be used to extend its content by effective operators, resulting from yet unknown new physics at higher energy scales, exploiting the fact that these higher energy effects do not have to be known explicitly. In this case, the Standard Model is seen as a low energy approximation of a hypothetical complete model. This application is then referred to as the *Standard Model Effective Field Theory* (SMEFT).

Due to redundancies, there exists some freedom in choosing how the effective operators are represented by using integration by parts, the equations of motion and Fierz identities. In SMEFT, one of the most widespread choices is the Warsaw basis [24], which is also the choice that will be used as the main reference in this thesis. Here, only dim-6 operators are used since dim-5 operators are associated to lepton number violation and are mostly used in neutrino physics. The full set of operators with a mass dimension of 6 can be seen in figure 1.3.

X^3		φ^6 and $\varphi^4 D^2$		$\psi^2\varphi^3$	
Q_G	$f^{ABC}G_\mu^{A\nu}G_\nu^{B\rho}G_\rho^{C\mu}$	Q_φ	$(\varphi^\dagger\varphi)^3$	$Q_{e\varphi}$	$(\varphi^\dagger\varphi)(\bar{l}_p e_r\varphi)$
$Q_{\widetilde{G}}$	$f^{ABC}\widetilde{G}_\mu^{A\nu}G_\nu^{B\rho}G_\rho^{C\mu}$	$Q_{\varphi\Box}$	$(\varphi^\dagger\varphi)\Box(\varphi^\dagger\varphi)$	$Q_{u\varphi}$	$(\varphi^\dagger\varphi)(\bar{q}_p u_r\widetilde{\varphi})$
Q_W	$\varepsilon^{IJK}W_\mu^{I\nu}W_\nu^{J\rho}W_\rho^{K\mu}$	$Q_{\varphi D}$	$\left(\varphi^\dagger D^\mu\varphi\right)^\star\left(\varphi^\dagger D_\mu\varphi\right)$	$Q_{d\varphi}$	$(\varphi^\dagger\varphi)(\bar{q}_p d_r\varphi)$
$Q_{\widetilde{W}}$	$\varepsilon^{IJK}\widetilde{W}_\mu^{I\nu}W_\nu^{J\rho}W_\rho^{K\mu}$				

$X^2\varphi^2$		$\psi^2 X\varphi$		$\psi^2\varphi^2 D$	
$Q_{\varphi G}$	$\varphi^\dagger\varphi\, G_{\mu\nu}^A G^{A\mu\nu}$	Q_{eW}	$(\bar{l}_p\sigma^{\mu\nu}e_r)\tau^I\varphi W_{\mu\nu}^I$	$Q_{\varphi l}^{(1)}$	$(\varphi^\dagger i\overleftrightarrow{D}_\mu\varphi)(\bar{l}_p\gamma^\mu l_r)$
$Q_{\varphi\widetilde{G}}$	$\varphi^\dagger\varphi\,\widetilde{G}_{\mu\nu}^A G^{A\mu\nu}$	Q_{eB}	$(\bar{l}_p\sigma^{\mu\nu}e_r)\varphi B_{\mu\nu}$	$Q_{\varphi l}^{(3)}$	$(\varphi^\dagger i\overleftrightarrow{D}_\mu^I\varphi)(\bar{l}_p\tau^I\gamma^\mu l_r)$
$Q_{\varphi W}$	$\varphi^\dagger\varphi\, W_{\mu\nu}^I W^{I\mu\nu}$	Q_{uG}	$(\bar{q}_p\sigma^{\mu\nu}T^A u_r)\widetilde{\varphi}\, G_{\mu\nu}^A$	$Q_{\varphi e}$	$(\varphi^\dagger i\overleftrightarrow{D}_\mu\varphi)(\bar{e}_p\gamma^\mu e_r)$
$Q_{\varphi\widetilde{W}}$	$\varphi^\dagger\varphi\,\widetilde{W}_{\mu\nu}^I W^{I\mu\nu}$	Q_{uW}	$(\bar{q}_p\sigma^{\mu\nu}u_r)\tau^I\widetilde{\varphi}\, W_{\mu\nu}^I$	$Q_{\varphi q}^{(1)}$	$(\varphi^\dagger i\overleftrightarrow{D}_\mu\varphi)(\bar{q}_p\gamma^\mu q_r)$
$Q_{\varphi B}$	$\varphi^\dagger\varphi\, B_{\mu\nu}B^{\mu\nu}$	Q_{uB}	$(\bar{q}_p\sigma^{\mu\nu}u_r)\widetilde{\varphi}\, B_{\mu\nu}$	$Q_{\varphi q}^{(3)}$	$(\varphi^\dagger i\overleftrightarrow{D}_\mu^I\varphi)(\bar{q}_p\tau^I\gamma^\mu q_r)$
$Q_{\varphi\widetilde{B}}$	$\varphi^\dagger\varphi\,\widetilde{B}_{\mu\nu}B^{\mu\nu}$	Q_{dG}	$(\bar{q}_p\sigma^{\mu\nu}T^A d_r)\varphi\, G_{\mu\nu}^A$	$Q_{\varphi u}$	$(\varphi^\dagger i\overleftrightarrow{D}_\mu\varphi)(\bar{u}_p\gamma^\mu u_r)$
$Q_{\varphi WB}$	$\varphi^\dagger\tau^I\varphi\, W_{\mu\nu}^I B^{\mu\nu}$	Q_{dW}	$(\bar{q}_p\sigma^{\mu\nu}d_r)\tau^I\varphi\, W_{\mu\nu}^I$	$Q_{\varphi d}$	$(\varphi^\dagger i\overleftrightarrow{D}_\mu\varphi)(\bar{d}_p\gamma^\mu d_r)$
$Q_{\varphi\widetilde{W}B}$	$\varphi^\dagger\tau^I\varphi\,\widetilde{W}_{\mu\nu}^I B^{\mu\nu}$	Q_{dB}	$(\bar{q}_p\sigma^{\mu\nu}d_r)\varphi\, B_{\mu\nu}$	$Q_{\varphi ud}$	$i(\widetilde{\varphi}^\dagger D_\mu\varphi)(\bar{u}_p\gamma^\mu d_r)$

$(\bar{L}L)(\bar{L}L)$		$(\bar{R}R)(\bar{R}R)$		$(\bar{L}L)(\bar{R}R)$	
Q_{ll}	$(\bar{l}_p\gamma_\mu l_r)(\bar{l}_s\gamma^\mu l_t)$	Q_{ee}	$(\bar{e}_p\gamma_\mu e_r)(\bar{e}_s\gamma^\mu e_t)$	Q_{le}	$(\bar{l}_p\gamma_\mu l_r)(\bar{e}_s\gamma^\mu e_t)$
$Q_{qq}^{(1)}$	$(\bar{q}_p\gamma_\mu q_r)(\bar{q}_s\gamma^\mu q_t)$	Q_{uu}	$(\bar{u}_p\gamma_\mu u_r)(\bar{u}_s\gamma^\mu u_t)$	Q_{lu}	$(\bar{l}_p\gamma_\mu l_r)(\bar{u}_s\gamma^\mu u_t)$
$Q_{qq}^{(3)}$	$(\bar{q}_p\gamma_\mu\tau^I q_r)(\bar{q}_s\gamma^\mu\tau^I q_t)$	Q_{dd}	$(\bar{d}_p\gamma_\mu d_r)(\bar{d}_s\gamma^\mu d_t)$	Q_{ld}	$(\bar{l}_p\gamma_\mu l_r)(\bar{d}_s\gamma^\mu d_t)$
$Q_{lq}^{(1)}$	$(\bar{l}_p\gamma_\mu l_r)(\bar{q}_s\gamma^\mu q_t)$	Q_{eu}	$(\bar{e}_p\gamma_\mu e_r)(\bar{u}_s\gamma^\mu u_t)$	Q_{qe}	$(\bar{q}_p\gamma_\mu q_r)(\bar{e}_s\gamma^\mu e_t)$
$Q_{lq}^{(3)}$	$(\bar{l}_p\gamma_\mu\tau^I l_r)(\bar{q}_s\gamma^\mu\tau^I q_t)$	Q_{ed}	$(\bar{e}_p\gamma_\mu e_r)(\bar{d}_s\gamma^\mu d_t)$	$Q_{qu}^{(1)}$	$(\bar{q}_p\gamma_\mu q_r)(\bar{u}_s\gamma^\mu u_t)$
		$Q_{ud}^{(1)}$	$(\bar{u}_p\gamma_\mu u_r)(\bar{d}_s\gamma^\mu d_t)$	$Q_{qu}^{(8)}$	$(\bar{q}_p\gamma_\mu T^A q_r)(\bar{u}_s\gamma^\mu T^A u_t)$
		$Q_{ud}^{(8)}$	$(\bar{u}_p\gamma_\mu T^A u_r)(\bar{d}_s\gamma^\mu T^A d_t)$	$Q_{qd}^{(1)}$	$(\bar{q}_p\gamma_\mu q_r)(\bar{d}_s\gamma^\mu d_t)$
				$Q_{qd}^{(8)}$	$(\bar{q}_p\gamma_\mu T^A q_r)(\bar{d}_s\gamma^\mu T^A d_t)$

$(\bar{L}R)(\bar{R}L)$ and $(\bar{L}R)(\bar{L}R)$		B-violating	
Q_{ledq}	$(\bar{l}_p^j e_r)(\bar{d}_s q_t^j)$	Q_{duq}	$\varepsilon^{\alpha\beta\gamma}\varepsilon_{jk}\left[(d_p^\alpha)^T C u_r^\beta\right]\left[(q_s^{\gamma j})^T C l_t^k\right]$
$Q_{quqd}^{(1)}$	$(\bar{q}_p^j u_r)\varepsilon_{jk}(\bar{q}_s^k d_t)$	Q_{qqu}	$\varepsilon^{\alpha\beta\gamma}\varepsilon_{jk}\left[(q_p^{\alpha j})^T C q_r^{\beta k}\right]\left[(u_s^\gamma)^T C e_t\right]$
$Q_{quqd}^{(8)}$	$(\bar{q}_p^j T^A u_r)\varepsilon_{jk}(\bar{q}_s^k T^A d_t)$	Q_{qqq}	$\varepsilon^{\alpha\beta\gamma}\varepsilon_{jn}\varepsilon_{km}\left[(q_p^{\alpha j})^T C q_r^{\beta k}\right]\left[(q_s^{\gamma m})^T C l_t^n\right]$
$Q_{lequ}^{(1)}$	$(\bar{l}_p^j e_r)\varepsilon_{jk}(\bar{q}_s^k u_t)$	Q_{duu}	$\varepsilon^{\alpha\beta\gamma}\left[(d_p^\alpha)^T C u_r^\beta\right]\left[(u_s^\gamma)^T C e_t\right]$
$Q_{lequ}^{(3)}$	$(\bar{l}_p^j\sigma_{\mu\nu}e_r)\varepsilon_{jk}(\bar{q}_s^k\sigma^{\mu\nu}u_t)$		

Figure 1.3.: The full set of dim-6 effective operators for SMEFT in the Warsaw basis, taken from [24].

1.4. Methodology and Notation

In order to obtain numerical results in the form of Monte Carlo simulations surrounding SMEFT phenomenology, the numerical event generator WHIZARD [25] is used, which allows parameters associated with the process to be set as well as changing further conditions relating to the interaction. The model itself is implemented using a version of the amplitude provider GOSAM [26] that has been modified for the intended inclusion of effective operators. It supplies the process with the required matrix elements up to NLO precision and allows a custom implementation of the physics model. The goal of this work is to document the additional development and validation process of the WHIZARD + GOSAM framework in order to numerically evaluate EFT processes at NLO. More on this framework in general is summarized in section 1.4.1.

During the project, a constant reference is made to the paper by Maltoni et al. [18] on $t\bar{t}H$ production in SMEFT. It acts as the main source of validation and inspiration for setting up the framework.

To describe $t\bar{t}H$ production by considering general proton-proton collisions in SMEFT, one typically includes three effective operators. By considering the Warsaw basis, these are

$$\mathcal{O}_{\mathrm{t}\varphi} = (\varphi^\dagger\varphi)(\bar{t}t\tilde{\varphi}) \qquad \mathcal{O}_{\varphi G} = \varphi^\dagger\varphi G^a_{\mu\nu}G^{a\,\mu\nu} \qquad \mathcal{O}_{\mathrm{t}G} = (\bar{t}\sigma^{\mu\nu}T^a t)\tilde{\varphi}G^a_{\mu\nu}\,,$$

all three of which are dim-6 operators. As can be seen, only the top quark will be used as the up-type fermionic part, since its presence, together with the Higgs boson, is the main feature of this study. Taking these into account, they will generally contribute to the cross section of the process at hand. Some possible insertions are shown schematically in figure 1.4. However, due to complications in the intended automation procedures, caused by the more complex Lorentz structure of the chromomagnetic operator $\mathcal{O}_{\mathrm{t}G}$, this thesis will mainly focus on $\mathcal{O}_{\mathrm{t}\varphi}$ and $\mathcal{O}_{\varphi G}$ as the relevant effective operators. Furthermore, the effective corrections will only be considered in the order of $\mathcal{O}(\Lambda^{-2})$ on amplitude level, which means that at most one effective operator will be included in any diagram (no double insertions). No dim-5 operators will be considered, as discussed in section 1.3. The higher order QCD corrections will be included up to $\mathcal{O}(\alpha_s)$, while no explicit QED corrections are considered. In addition, the corresponding Wilson coefficients are considered to be real-valued parameters. All quarks will be seen as massless except for the top quark.

The dimension of the operators and associated Wilson coefficients is always implicitly assumed to be $d = 6$, unless otherwise specified. For other quantities, the mass dimension is noted by the parentheses $[\dots]_m$.

Since the effective operators in [18] are defined with additional factors compared to those in the Warsaw basis, the convention is introduced to write $\mathcal{O}_i$ for the operators from the Warsaw basis, $\widetilde{\mathcal{O}}_i$ for those with generic additional factors (as defined further in section 2.1.3) and $\widetilde{O}_i^{\mathrm{M}}$ for the operators with the specific convention of Maltoni et al. Similar notation is adopted for the corresponding Wilson coefficients, counterterms etc. The differing convention is used in order to force all amplitudes to be of order $\mathcal{O}(\alpha_s\, y_t)$ at tree-level. For the sake of generality, all important results are therefore given in the generalized case.

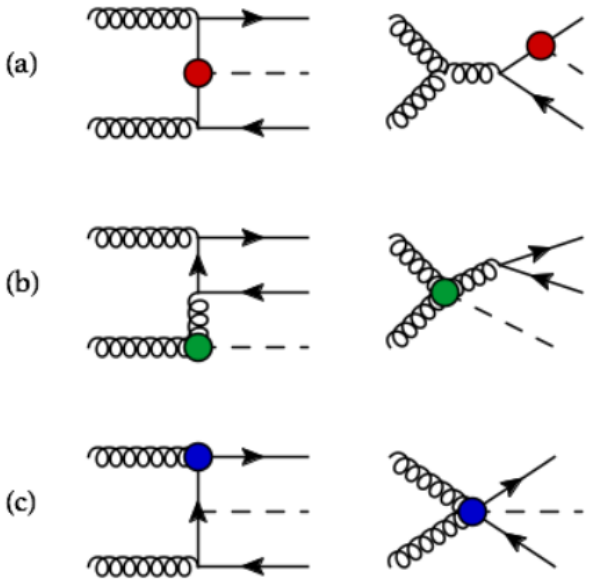

Figure 1.4.: Some examples of tree-level Feynman diagrams for $t\bar{t}H$ production, taken from [18]. The dots represent the operators (a): $\mathcal{O}_{t\varphi}$, (b): $\mathcal{O}_{\varphi G}$, (c): $\mathcal{O}_{tG}$.

1.4.1. WHIZARD + GOSAM Workflow

To outline the multiple necessary steps to get from the user input to the cross section, one starts at the runcard that the user must provide in the WHIZARD script language *Sindarin*. It defines all the details and the parameters of the process, such as the external particles, the beam energy, the physics model and so on. After reading in this information, WHIZARD first uses its own matrix element generator *O'Mega* to generate Fortran code, which contains the necessary metadata for the process at hand. The next step, in this case, is the call to GOSAM by the BLHA interface [27], which will check for and load all necessary programs for the matrix element generation. These include QGRAF (based on [28]) as the topology generator for the Feynman diagrams, FORM [29, 30] to perform symbolic algebra manipulations as well as one of SAMURAI [31], GOLEM95C [32] or NINJA [33] for the tensor reduction. For the evaluation of the loop integrals, ONELOOP [34] and QCDLOOP (based on [35]) can be used. Next, GOSAM communicatates with WHIZARD via BLHA files in order to ensure the correct generation of the process files based on the details from the *Sindarin* file. GOSAM then generates Fortran code that represents the different components of the process, which is then compiled and linked to a process library, which in turn is available to WHIZARD.

As soon as the process libraries are compiled and loaded, WHIZARD will initiate its random number generator TAO after which the Monte Carlo phase space generation and integration process will start, which is based on the VAMP package [36]. This yields the numerical results for the different contributions to the cross section (see chapter 3) together with the corresponding Monte Carlo errors. After this, WHIZARD also offers the option to generate simulated event samples.

2. Model Implementation

2.1. NLO SMEFT Effects

2.1.1. Renormalization

In quantum field theory, renormalization addresses the issue of divergences that arise when calculating loop diagrams beyond leading order perturbation theory. One can systematically modify the parameters of a theory in order to asborb these infinities, allowing for finite results. Here, the process will be relevant up to the first loop order in QCD, translating to an order of $\mathcal{O}(\alpha_S^3)$ in the squared amplitude, since there is an α_S dependence on tree-level. By explicitly writing the strong couplings, one can express the total unrenormalized NLO amplitude as

$$\mathcal{A}_0 = \alpha_{S,0}\,\mathcal{A}_0^{(0)} + \alpha_{S,0}^2\,\mathcal{A}_0^{(1)}\,,$$

where $\mathcal{A}^{(k)}$ is the amplitude for the k-loop diagrams. One can now use the renormalization constants and counterterms

$$\alpha_{S,0} = Z_\alpha\,\alpha_S \quad ; \qquad m_{t,0}^2 = m_t^2 + \alpha_S\,\delta m_t^2$$
$$Z_\alpha = 1 + \alpha_S\,\delta Z_\alpha \quad ; \quad Z_G = 1 + \alpha_S\,\delta Z_G\,\Delta_G \quad ; \quad Z_t = 1 + \alpha_S\,\delta Z_t\,,$$

in order to replace all bare quantities (with index 0) with their renormalized parts and cancel the UV divergencies (infinities at high energies). Only external fields need to be renormalized - and only the heavy quarks contained therein. The initial state contains protons, which consist of either light quarks ($\Delta_G = 0$) or gluons ($\Delta_G = 1$). The total renormalized amplitude can then be written as

$$\begin{aligned}\mathcal{A} &= Z_\alpha\,Z_G\,Z_t\left[\alpha_S\left(\mathcal{A}^{(0)} + \alpha_S\,\delta m_t^2\,\mathcal{A}_m^{(0)}\right) + Z_\alpha\,\alpha_S^2\,\mathcal{A}^{(1)}\right] + \mathcal{O}(\alpha_S^3) \\ &= \alpha_S\left[1+\alpha_S\,\delta Z_\alpha\right]\left[1+\alpha_S\,\delta Z_G\,\Delta_G\right]\left[1+\alpha_S\,\delta Z_t\right]\mathcal{A}^{(0)} \\ &+ \alpha_S^2\left[1+\alpha_S\,\delta Z_\alpha\right]^2\left[1+\alpha_S\,\delta Z_G\,\Delta_G\right]\left[1+\alpha_S\,\delta Z_t\right]\mathcal{A}^{(1)} \\ &+ \alpha_S^2\,\delta m_t^2\,\mathcal{A}_m^{(0)} + \mathcal{O}(\alpha_S^3)\,,\end{aligned} \tag{2.1}$$

where $\mathcal{A}_m$ is the derivative term of the amplitude after an expansion in $\alpha_S\,\delta m_t^2$. By squaring the amplitude and only keeping the desired orders of α_S, one arrives at

$$\begin{aligned}|\mathcal{A}|^2 &= \mathcal{A}^\dagger\mathcal{A} \\ &= \alpha_S^2\,|\mathcal{A}^{(0)}|^2 + 2\,\alpha_S^3\,|\mathcal{A}^{(0)}|^2\left[\delta Z_\alpha + \delta Z_G\,\Delta_G + \delta Z_t\right] \\ &+ \alpha_S^3\left(\mathcal{A}^{\dagger\,(0)}\mathcal{A}_m^{(0)} + \text{h.c.}\right)\delta m_t^2 + \alpha_S^3\left(\mathcal{A}^{\dagger\,(1)}\mathcal{A}^{(0)} + \text{h.c.}\right) + \mathcal{O}(\alpha_S^4)\,.\end{aligned} \tag{2.2}$$

After this general renormalization, one can also do the same with explicit effective operators, basically extending the previous expression by using the full SMEFT amplitude

$$\mathcal{B}_0 = \alpha_{S,0}\,\overline{\mathcal{B}}_0^{(0)} + \alpha_{S,0}^2\,\overline{\mathcal{B}}_0^{(1)} \tag{2.3}$$

$$\overline{\mathcal{B}}_0^{(k)} := \mathcal{A}_0^{(k)} + \sum_i \frac{C_{0,i}}{\Lambda^2}\,\mathcal{B}_{i,0}^{(k)}\ . \tag{2.4}$$

Define the renormalization of the Wilson coefficients by

$$C_{0,i} = Z_{ij}\,C_j = (1 + \alpha_S\,\delta Z_{ij})\,C_j\ .$$

In the same way as before, the renormalized amplitude for the SMEFT scenario results into

$$\begin{aligned}|\mathcal{B}|^2 = |\mathcal{A}|^2 + \alpha_S^2\Bigg(&\Bigg\{\left[\frac{1}{2}\,\Sigma_B^{\dagger\,(0)}\Sigma_B^{(0)} + \mathcal{A}^{\dagger\,(0)}\Sigma_B^{(0)}\right]\Big(1 + \alpha_S\,2\,[\delta Z_\alpha + \delta Z_G\,\Delta_G + \delta Z_t]\Big)\\ &+ \alpha_S\left[\Sigma_B^{\dagger\,(0)}\delta\,\Sigma_B^{(0)} + \mathcal{A}^{\dagger\,(0)}\delta\,\Sigma_B^{(0)}\right]\\ &+ \alpha_S\,\delta m_t^2\left[\mathcal{A}_m^{\dagger\,(0)}\Sigma_B^{(0)} + \Sigma_B^{\dagger\,(0)}\Sigma_{B_m}^{(0)} + \mathcal{A}^{\dagger\,(0)}\Sigma_{B_m}^{(0)}\right]\\ &+ \alpha_S\left[\mathcal{A}^{\dagger\,(1)}\Sigma_B^{(0)} + \Sigma_B^{\dagger\,(0)}\Sigma_B^{(1)} + \mathcal{A}^{\dagger\,(0)}\Sigma_B^{(1)}\right]\Bigg\} + \text{h. c.}\Bigg)\\ &+ \mathcal{O}(\alpha_S^4)\ ,\end{aligned} \tag{2.5}$$

where the definitions

$$\Sigma_B^{(k)} := \sum_i \frac{C_i}{\Lambda^2}\,\mathcal{B}_i^{(k)} \quad ; \qquad \delta\,\Sigma_B^{(k)} := \sum_i \frac{\delta Z_{ij}\,C_j}{\Lambda^2}\,\mathcal{B}_i^{(k)}\ ,$$

have been used. Equation 2.5 contains terms proportional to Λ^{-4}, which are kept since they come purely from squaring the amplitude. By identifying the actual renormalized amplitude per loop order, based on definition 2.4, one can write this in the more compact form

$$\begin{aligned}|\mathcal{B}|^2 = \alpha_S^2\Bigg\{&|\overline{\mathcal{B}}^{(0)}|^2\Big(1 + \alpha_S\,2\sum_k \delta Z_k\Big) + \alpha_S\left[\overline{\mathcal{B}}^{\dagger\,(0)}\,\delta\,\Sigma_B^{(0)} + \text{h.c.}\right]\\ &+ \alpha_S\,\delta m_t^2\left[\overline{\mathcal{B}}_m^{\dagger\,(0)}\,\overline{\mathcal{B}}^{(0)} + \text{h.c.}\right] + \alpha_S\left[\overline{\mathcal{B}}^{\dagger\,(1)}\,\overline{\mathcal{B}}^{(0)} + \text{h.c.}\right]\Bigg\} + \mathcal{O}(\alpha_S^4)\ .\end{aligned} \tag{2.6}$$

This, however, can actually be written in terms of the previous result from equation 2.2

$$|\mathcal{B}|^2 = |\mathcal{A}|^2\Big|_{\mathcal{A}^{(k)}\to\overline{\mathcal{B}}^{(k)}} + \Delta\mathcal{C}\ , \tag{2.7}$$

where the amplitude $\mathcal{A}$ is replaced with with $\overline{\mathcal{B}}^{(k)}$ in the first term. The additional term $\Delta\mathcal{C}$ comes purely from the renormalization of the Wilson coefficients

$$\Delta\mathcal{C} = \alpha_S^3\left[\overline{\mathcal{B}}^{\dagger\,(0)}\,\delta\,\Sigma_B^{(0)} + \text{h.c.}\right]\ .$$

This means that the usual renormalization procedure for the SM can be completely kept where only an additional additive correction term is needed, which is helpful when working with automated amplitude providers as it makes the renormalization procedure for a SMEFT theory more straightforward and consistent.

2.1.2. Redefinitions

The effective Operators considered in this thesis can modify the prefactors of SM terms when contributing a combination of fields already present in the SM. When this happens for the kinetic or mass terms of the Lagrangian, one needs to redefine certain parameters to maintain the same (canonical) form as before in order to ensure that the theoretical predictions retain the same validity. To see this effect, consider the operator

$$\mathcal{O}_{t\varphi} = (\varphi^\dagger \varphi)\, \bar{t}\, t\, \tilde{\varphi}\ .$$

After the SSB, this operator produces a term proportional to $\bar{t}\, t$, which will change the mass structure of the top quark to the following term

$$\mathcal{L}_{SMEFT} \supset \left(m_t + \frac{C_{t\varphi}\, v^3}{2\sqrt{2}\, \Lambda^2} \right) \bar{t}\, t\ . \tag{2.8}$$

To compensate this modification, the top-mass has to be redefined to

$$m_t \to m_t' = m_t + \frac{C_{t\varphi}\, v^3}{2\sqrt{2}\, \Lambda^2}\ . \tag{2.9}$$

Re-expressing all other top-masses in terms of m_t' will then result into a modification of other interaction terms. This is to be expected as the effective operators describe additional ways for the fields to interact. However, the redefinition also fixates the mass term to the desired canonical form $m_t'\, t\bar{t}$.

Similarly, the operator $\mathcal{O}_{\varphi G}$ produces a term

$$\mathcal{O}_{\varphi G} \supset \frac{C_{\varphi G}\, v^2}{2}\, G^a_{\mu\nu} G^{a\,\mu\nu}\ ,$$

which will change the kinetic gluon structure to the following

$$\mathcal{L}_{SMEFT} \supset -\frac{1}{4}\, G^a_{\mu\nu} G^{a\,\mu\nu} \left(1 - 2\, v^2\, \frac{C_{\varphi G}}{\Lambda^2} \right)\ . \tag{2.10}$$

To remove the additional factor, one can adjust the gluon fields to

$$G^a_\mu \to G'^a_\mu = G^a_\mu \left(1 + v^2\, \frac{C_{\varphi G}}{\Lambda^2} \right)\ . \tag{2.11}$$

This will raise the effective contributions of the kinetic terms to the order $\mathcal{O}(\Lambda^{-4})$ in the SMEFT Lagrangian, which are subsequently truncated and neglected. However, this redefinition will not address the issue completely. The first remaining problem is the fact that this will not correctly normalize the $\sim G^a_\mu G^a_\nu$ terms coming from $G^a_{\mu\nu}$. The second problem is that the redefinition will also propagate to the covariant derivative, which will therefore change the kinetic structure of quarks. Both can be solved by also introducing a redefined strong coupling constant with

$$g_s \to g_s' = g_s \left(1 - v^2\, \frac{C_{\varphi G}}{\Lambda^2} \right)\ , \tag{2.12}$$

which suppresses the additional contributions in the same way as equation 2.11 does.

The third operator, $\mathcal{O}_{tG}$, does not contain any potential duplicate field structures from the SM and will therefore not contribute to any further redefinition.

2.1.3. Operator Mixing and Renormalization Group Equations

When renormalizing the introduced effective operators, one generally encounters the possibility of mixing between different operators at a higher order, which will also expose this mixing into the Renormalization Group Equations (RGEs) of the model (see e.g. [37]). Consider the form

$$\mathcal{O}_{0,i}^{(k)} = \sum_j Z_{ij}^{(k)}(\mu)\, \mathcal{O}_j^{(k)}(\mu)\ . \tag{2.13}$$

Here, μ is the renormalization scale. The unrenormalized operator $\mathcal{O}_{0,i}^{(k)}$ needs to be independent of this scale, which means that one can write

$$\begin{aligned} &\sum_j \left[\frac{\mathrm{d}Z_{ij}^{(k)}(\mu)}{\mathrm{d}\ln(\mu)}\, \mathcal{O}_j^{(k)}(\mu) + Z_{ij}^{(k)}(\mu)\, \frac{\mathrm{d}\mathcal{O}_j^{(k)}(\mu)}{\mathrm{d}\ln(\mu)} \right] = 0 \\ \Rightarrow &\sum_j Z_{ij}^{(k)}(\mu)\, \frac{\mathrm{d}\mathcal{O}_j^{(k)}(\mu)}{\mathrm{d}\ln(\mu)} = -\sum_j \frac{\mathrm{d}Z_{ij}^{(k)}(\mu)}{\mathrm{d}\ln(\mu)}\, \mathcal{O}_j^{(k)}(\mu)\ . \end{aligned}$$

To single out one of the operators on one side, expand both sides of the equation by $Z_{ni}^{-1\,(k)}(\mu)$ and sum over i. This then leads to

$$\frac{\mathrm{d}\mathcal{O}_n^{(k)}(\mu)}{\mathrm{d}\ln(\mu)} = -\sum_{i,j} Z_{ni}^{-1\,(k)}(\mu)\, \frac{\mathrm{d}Z_{ij}^{(k)}(\mu)}{\mathrm{d}\ln(\mu)}\, \mathcal{O}_j^{(k)}(\mu) := -\sum_j \tilde{\gamma}_{nj}\, \mathcal{O}_j^{(k)}\ . \tag{2.14}$$

In the last step, the matrix $\tilde{\gamma}$ has been introduced, which is called the anomalous dimension matrix. One can also extend this logic to the Wilson coefficients by using the fact that the total Lagrangian of the model should be scale independent

$$\begin{aligned} &\sum_i \left[\frac{\mathrm{d}C_i^{(k)}(\mu)}{\mathrm{d}\ln(\mu)}\, \mathcal{O}_i^{(k)}(\mu) + C_i^{(k)}(\mu)\, \frac{\mathrm{d}\mathcal{O}_i^{(k)}(\mu)}{\mathrm{d}\ln(\mu)} \right] = 0 \\ \Rightarrow\ &\frac{\mathrm{d}C_j^{(k)}(\mu)}{\mathrm{d}\ln(\mu)} = \sum_i C_i^{(k)}(\mu)\, \tilde{\gamma}_{ij} := \sum_i \gamma_{ji}\, C_i^{(k)}(\mu)\ , \end{aligned} \tag{2.15}$$

where $\gamma = \tilde{\gamma}^T$ is the anomalous dimension matrix of the Wilson coefficients. Thus, this matrix can be determined by knowing the renormalization constants of the effective operators. The resulting equations between the scale-derivatives and linear combinations of the Wilson coefficients are the RGEs. These are already known for this case and are collected in [38–40].

By only focusing on $C_{\mathrm{t}\varphi}$, $C_{\varphi G}$ and $C_{\mathrm{t}G}$, as well as using real valued Wilson coefficients and setting $c_{F,3} = 8/6$, one retrieves the following RGEs from the collection mentioned above

$$\begin{aligned} \dot{C}_{\mathrm{t}\varphi} \ &= C_{\mathrm{t}\varphi}\Big[y_t^2\, \tfrac{45}{2} - g_s^2 \cdot 8 + \dots\Big] + C_{\varphi G}\Big[g_s^2 y_t \cdot 32\Big] \qquad\qquad + C_{\mathrm{t}G}\Big[-g_s y_t^2 \cdot 32\Big] \\ \dot{C}_{\varphi G} = \ &\qquad + C_{\varphi G}\Big[y_t^2 \cdot 6 - g_s^2 \cdot 14 + \dots\Big] + C_{\mathrm{t}G}\Big[-g_s y_t \cdot 4\Big] \\ \dot{C}_{\mathrm{t}G} \ = \ &\qquad + C_{\varphi G}\Big[-g_s y_t \cdot 4\Big] \qquad\qquad + C_{\mathrm{t}G}\Big[y_t^2\, \tfrac{15}{2} - g_s^2\, \tfrac{17}{3} + \dots\Big]\ , \end{aligned}$$

where the ellipsis represents other terms with electroweak couplings or parameters that are not relevant in this context, since they will not be used in perturbative expansions. As introduced in [39], the $\dot{C}_i$ symbols are defined as

$$\dot{C}_i = 16\pi^2 \frac{\mathrm{d}}{\mathrm{d}\ln(\mu)} C_i \,. \tag{2.16}$$

If one wants to define the effective operators with additional factors (including powers of g_s and y_t), a generalized Wilson coefficient can be written as

$$\widetilde{C}_i = x_i \, y_t^{a_i} g_s^{b_i} \cdot C_i \,, \tag{2.17}$$

where x_i can be any real valued constant. The parameters x_i, a_i and b_i should then be chosen such that they cancel all additional factors in the corresponding operator definition. In order to produce the adjusted RGEs with the coefficients as in 2.17, one can write

$$\dot{\widetilde{C}}_i = \left(a_i \cdot \frac{\dot{y}_t}{y_t} + b_i \cdot \frac{\dot{g}_s}{g_s} \right) \cdot x_i \, y_t^{a_i} g_s^{b_i} \cdot C_i + x_i \, y_t^{a_i} g_s^{b_i} \cdot \dot{C}_i \,. \tag{2.18}$$

The anomalous coupling terms are given by the SM as

$$\frac{\dot{y}_t}{y_t} = \vartheta \cdot \left(\frac{9}{2} \cdot y_t^2 - 8\, g_s^2 \right) \quad , \qquad \frac{\dot{g}_s}{g_s} = -7\, g_s^2 \,,$$

with $\vartheta = 1$. According to [38], there will also be contributions of the form $\dot{y}_t \sim C_{\mathrm{t}\varphi}$ and $\dot{g}_s \sim C_{\varphi G}$, however, since these lead to double insertion terms, they can be neglected. Inserting these coupling terms into the adjusted RG equations 2.18, as well as replacing $\dot{C}_i$ with the known RGEs of the unaltered Wilson coefficients from above, this will result into the following generalized Wilson coefficient RGEs

$$\begin{aligned}
\dot{\widetilde{C}}_{\mathrm{t}\varphi} \;&= \widetilde{C}_{\mathrm{t}\varphi} \left[y_t^2 \tfrac{45}{2} - g_s^2 \cdot 8 + \kappa_1 \right] + \widetilde{C}_{\varphi G} \left[32 \tfrac{x_1}{x_2} \, y_t^{a_1 - a_2 + 1} \, g_s^{b_1 - b_2 + 2} \right] - \widetilde{C}_{\mathrm{t}G} \left[32 \tfrac{x_1}{x_3} \, y_t^{a_1 - a_3 + 2} \, g_s^{b_1 - b_3 + 1} \right] \\
\dot{\widetilde{C}}_{\varphi G} = \;& + \widetilde{C}_{\varphi G} \left[y_t^2 \cdot 6 - g_s^2 \cdot 14 + \kappa_2 \right] \quad - \widetilde{C}_{\mathrm{t}G} \left[4 \tfrac{x_2}{x_3} \, y_t^{a_2 - a_3 + 1} \, g_s^{b_2 - b_3 + 1} \right] \\
\dot{\widetilde{C}}_{\mathrm{t}G} \;=\; & - \widetilde{C}_{\varphi G} \left[4 \tfrac{x_3}{x_2} \, y_t^{a_3 - a_2 + 1} \, g_s^{b_3 - b_2 + 1} \right] + \widetilde{C}_{\mathrm{t}G} \left[y_t^2 \tfrac{15}{2} - g_s^2 \tfrac{17}{3} + \kappa_3 \right] ,
\end{aligned}$$

with

$$\kappa_i = y_t^2 \, \vartheta \, a_i \, \frac{9}{2} - g_s^2 \left(8 \, \vartheta \, a_i + 7 \, b_i \right) \,.$$

The $\mathrm{t}G, \varphi\mathrm{G}$ component will vanish from the results later on (section 2.4). This is because only the terms proportional to g_s^2 are kept, due to the perturbative QCD expansion in $\mathcal{O}(\alpha_s)$. With the setup used, this is the only component that does not contribute such terms.

2.1.4. Wilson Coefficient Counterterms with Scheme Dependence

The renormalization procedure and thus also the counterterms of the Wilson coefficients are linked to the anomalous dimension matrix, as shown in equation 2.14 and 2.15. However, a more practical approach to obtain an identical relation can be applied as follows: Define the counterterms for the Wilson coefficients as

$$C_{0,i} = Z_{ij}\, C_j = (1 + \alpha_s \delta Z_{ij})\, C_j \ ,$$

where summation over equal indices is implied. By now taking the derivative on both sides with respect to $\ln(\mu)$ as defined in equation 2.16, one obtains

$$0 = \dot{Z}_{ij}\, C_j + Z_{ij}\, \dot{C}_j = \dot{Z}_{ij}\, C_j + Z_{ij} \gamma_{j,k}\, C_k \ . \tag{2.19}$$

Due to the used derivative, α_s behaves as

$$\dot{\alpha}_s = 16\pi^2\, \beta(\alpha_s) = -32\pi^2 \alpha_s\, \varepsilon - 56\pi \alpha_s^2 + \mathcal{O}(\alpha_s^3) \ .$$

Since the EFT scale dependence is fully contained in α_s, the derivative of the renormalization factor can be written as follows

$$\dot{Z}_{ij} = \dot{\alpha}_s\, \delta Z_{ij} = -32\pi^2 \alpha_s\, \varepsilon\, \delta Z_{ij} + \mathcal{O}(\alpha_s^2) \ ,$$

where only the sub-term from δZ_{ij} proportional to the ε^{-1} pole remains, since constant terms will be $\mathcal{O}(\varepsilon)$ in total. Let $\delta^{(-1)} Z_{ij}$ be the part of the counterterm proportional to ε^{-1}. Now insert everything back into equation 2.19 and expand γ_{ij} in orders of α_s to obtain

$$\gamma_{ij} = 32\pi^2 \alpha_s\, \delta^{(-1)} Z_{ij} + \mathcal{O}(\alpha_s^2) \ . \tag{2.20}$$

The combination $\Delta(\varepsilon)\, \delta^{(-1)} Z_{ij}$ is then identical to the $\overline{MS}$ counterterm of the Wilson coefficients in the 't Hooft Veltman (HV) scheme, which in turn is identical to the Conventional Dimensional Regularization (CDR) scheme at one loop calculations. Here, $\Delta(\varepsilon)$ is a variation of the usual factor that appears in dimensional regularization

$$\Delta(\varepsilon) = \frac{(4\pi)^\varepsilon}{\varepsilon} \frac{\Gamma^2(1-\varepsilon)\, \Gamma(1+\varepsilon)}{\Gamma(1-2\varepsilon)} \ .$$

However, GoSam uses the Dimensional Reduction (DRED) scheme by default for all SM parameters. Therefore, in order to implement the counterterms for the Wilson coefficient coherently into the custom model, it is required to know the (finite) shifts between the HV/CDR and DRED scheme, which will be written as $\delta^{\mathrm{D}RED} Z_{ij}$. Consequently, the total counterterm in this case can be written as

$$\delta Z_{ij} = \begin{cases} \Delta(\varepsilon)\, \delta^{(-1)} Z_{ij} & \text{, when working in the HV/CDR scheme} \\ \Delta(\varepsilon)\, \delta^{(-1)} Z_{ij} + \delta^{\mathrm{D}RED} Z_{ij} & \text{, when working in the DRED scheme} \end{cases} \tag{2.21}$$

The HV/CDR part is already known due to the results in chapter 2.1.3 and equation 2.20.

The DRED shifts can be obtained by renormalizing the Wilson coefficients in Dimensional Regularization and treating the dimension as a different variable, depending on where it originates. A distinction is necessary between the dimension in the loop integral and the dimensional dependencies occurring in the Dirac algebra. In the HV/CDR scheme, one then sets both dimensions identically to $d \equiv 4 - 2\varepsilon$. In DRED the Dirac algebra is performed in $\bar{d} = 4$ dimensions while the loop integration remains in d dimensions. The difference between both choices in the dimension $\bar{d}$ of the Dirac algebra represents the shift $\delta^{\mathrm{D}RED} Z_{ij}$.

Similar to what has been done in chapter 2.1.3, the counterterms can also be expressed in the context of generalized Wilson coefficients. By using the definition in equation 2.17, the renormalization is performed as

$$\widetilde{C}_{0,i} = x_i \, y_{t,0}^{a_i} \, g_{s,0}^{b_i} \cdot C_{0,i} = x_i \, \left(Z_y \, y_t\right)^{a_i} \left(Z_g \, g_s\right)^{b_i} \cdot Z_{ij} \, C_j = \frac{x_i}{x_j} \, y_t^{a_i - a_j} g_s^{b_i - b_j} \, Z_y^{a_i} Z_g^{b_i} Z_{ij} \, \widetilde{C}_j \; .$$

The expression in front of the renormalized $\widetilde{C}_j$ must be the renormalization factor in the generalized case, which is how one can identify

$$\widetilde{Z}_{ij} = \frac{x_i}{x_j} \, y_t^{a_i - a_j} g_s^{b_i - b_j} \, Z_y^{a_i} Z_g^{b_i} Z_{ij} \; . \tag{2.22}$$

By now expanding the renormalization factors and truncating the expression at the first order correction terms, equation 2.22 yields

$$\begin{aligned} \delta_{ij} + \delta\widetilde{Z}_{ij} &= \frac{x_i}{x_j} \, y_t^{a_i - a_j} g_s^{b_i - b_j} \; \left(1 + \delta Z_y\right)^{a_i} \left(1 + \delta Z_g\right)^{b_j} \left(\delta_{ij} + \delta Z_{ij}\right) \\ &\eqsim \frac{x_i}{x_j} \, y_t^{a_i - a_j} g_s^{b_i - b_j} \; \left(\delta_{ij} \left[1 + a_i \, \delta Z_y + b_i \, \delta Z_g\right] + \delta Z_{ij}\right) \\ &= \delta_{ij} + \delta_{ij} \left[a_i \, \delta Z_y + b_i \, \delta Z_g\right] + \frac{x_i}{x_j} \, y_t^{a_i - a_j} g_s^{b_i - b_j} \, \delta Z_{ij} \; . \end{aligned} \tag{2.23}$$

Each counterterm in this expression is to be understood as a total counterterm with the corresponding scheme dependence, like the one defined in equation 2.21. So by knowing the original counterterms (including potentially the DRED shift), one can use this formula to get the generalized counterterm.

The original counterterms of the Wilson coefficients can be obtained by extracting the UV poles from the typically associated one-loop correction diagrams of the corresponding operators, while also using the dimensional disctinction in order to identify the DRED shift. The mixing has to be taken into account by including all effective operators that contribute to the relevant Feynman-diagrams. The renormalization will be performed by using the $\overline{MS}$-scheme. This will lead to the counterterms of $\mathcal{O}_{\mathrm{t}\varphi}$, by considering the one-loop $t\bar{t}H$-vertex, and $\mathcal{O}_{\varphi G}$, by using the one-loop Hgg-vertex. The DRED shifts obtained in this way are

$$\delta^{\mathrm{D}RED} Z_{\mathrm{t}\varphi,t\varphi} = -\frac{1}{4\pi} \frac{4}{3} \qquad \delta^{\mathrm{D}RED} Z_{\mathrm{t}\varphi,\varphi G} = \frac{1}{4\pi} \frac{16}{3} \, y_t \tag{2.24}$$

$$\delta^{\mathrm{D}RED} Z_{\varphi G,t\varphi} = 0 \qquad \delta^{\mathrm{D}RED} Z_{\varphi G,\varphi G} = \frac{1}{4\pi} \qquad , \tag{2.25}$$

while the HV/CDR part can be reconstructed by using the combination of chapter 2.1.3 and equation 2.20, which yields the same result as with the procedure described above.

2.2. UFO Model Files

In order to implement a custom physics model for GoSam, so that the amplitude creation can be based on it, one can use the UFO (Universal FeynRules Output) format [41, 42]. This is a collection of Python files that define all the parameters, particles, couplings/vertices and structures that will be used in the model it describes. Such a model is created by using FeynRules [43] in combination with SmeftFR [44], where the latter is a special implementation for FeynRules in order to include SMEFT logic and export the model to the UFO format.

In the context of this thesis, a model with the Operators $\mathcal{O}_{t\varphi}$ and $\mathcal{O}_{\varphi G}$ has been created in this manner. More specifics on the parameter choices are given in the setup section 2.4. However, due to the need for increased customization and numerical efficiency, the UFO files are further modified after their automatic creation to provide a simplified and more target-oriented version. For this purpose, a custom Python script is used which automates the following:

- Remove redundant parameters: The creation of the UFO files also introduces some parameters that are not used in the model. These are removed.
- Remove unused parameters: Couplings that will evaluate to zero due to the chosen conditions and requirements, can also be completely removed since they will not contribute. These include e.g. Higgs couplings with light quarks, (anomalous) gluon couplings with light quarks, mixing quark structures in which fermion lines change their flavor, ...
- Add implicit couplings and factors: The additional g_s and y_t coupling constants as well as additional numerical factors which arise due to the definition of the effective operators should also be added explicitly to the feynman rules of the implemented couplings. The QCD and QED orders of the vertices are also changed accordingly.
- Fix the sign conventions: In order to be consistent with reference results as well as correcting internal sign mismatches, the different sign conventions need to be acknowledged and partially adapted. More on this in section 2.3.
- Separate and split up NP couplings/vertices: Couplings which contain SMEFT contributions have a new physics (NP) order. To circumvent problems with ambivalent vertices (those who have the same particle content but different couplings due to possible SM and SMEFT realizations) can be seperated and listed individually, sorted based on their NP order.
- Make all parameters real: The created UFO files define a lot of parameters as general complex-valued quantities. This overgeneralization can hinder the calculation process in the Whizard + GoSam framework, which is why it is ensured that every parameter is real-valued.

SmeftFR already consideres the necessary redefinitions discussed in section 2.1.2, which is why this does not have to be included manually. The additional counterterms for the Wilson coefficients and the corresponding renormalization parameters, however, have to be defined and included by hand, for which the UFO format also has implementation features [42]. The specific counterterm implementations are discussed in the setup section 2.4.

2.3. Sign conventions

There are mainly two signs that propagate through the calculations and can make some complications. The first one being the sign associated with the ghost sector of the Standard Model. The automatically created UFO model uses a different sign than GoSam assumes to correctly assign the propagator to the ghost particles. This has been identified due to the failure of pole cancellation in specific cases. This particular sign can be uniquely identified by comparing the coupling terms from the UFO's couplings.py file with a resource of general Feynman rules [22]. By looking at the $[\mathrm{gh}_{W^-}\,\overline{\mathrm{gh}}_{W^-}\,H]$ - vertex for example, it is clear that the UFO model in this case uses the convention $\eta_G^{UFO} = -1$, where $\eta_G \in \{1, -1\}$ is the general ghost sign convention used in [22]. For internal processes, GoSam assumes $\eta_G^{GS} = 1$. As this is incompatible, all couplings in the UFO model are modified in order to satisfy $\eta_G^{UFO} = \eta_G^{GS} = 1$.

The second sign η_s is the one coming from the covariant derivative, which also manifests itself in the $\mathrm{SU}(3)$ gauge group of the SM

$$D_\mu = \partial_\mu + i\eta_s g_s G_\mu^a T^a \tag{2.26}$$

$$G_{\mu\nu}^a = \partial_\mu G_\nu^a - \partial_\nu G_\mu^a - \eta_s g_s f^{abc} G_\mu^b G_\nu^c \,, \tag{2.27}$$

as shown in [22]. This then introduces the sign dependence into the $\mathcal{O}_{\varphi G}$ and $\mathcal{O}_{\mathrm{t}G}$ operators via the field strength tensors of the gluons. By inserting equation 2.27 into the operators, one can immediately see that η_s only appears in the terms proportional to $(\partial_\mu G_\nu^a) G^{b\,\mu} G^{c\,\nu}$ in $\mathcal{O}_{\varphi G}$ as well as the term proportional to $G_\mu^b G_\nu^c$ in $\mathcal{O}_{\mathrm{t}G}$. The former then corresponds to $ggg h$ and $gggh h$ vertices (the ggg vertex contribution of $\mathcal{O}_{\varphi G}$ is hidden in the redefinition of the gluon structure, as shown in section 2.1.2) while the latter represents the $t\bar{t}gg$ and $t\bar{t}ggh$ vertices. Equations 2.26 and 2.27 reveal that the only SM vertices where η_s appears are the $q\bar{q}g$, ggg and ghost-gluon vertices.

Due to the two covariant definitions from above, it becomes clear that each vertex with an η_s dependence, also comes with exactly one g_s, since both parameters exclusively appear together at the same order. Since all relevant tree-level processes are of order $\mathcal{O}(g_s^2)$, this means the sign η_s also only appears as a squared value and will not make a difference. However, the operator $\widetilde{\mathcal{O}}_{\mathrm{t}G}$ makes the potential exception since it is defined with an additional g_s factor in [18]. Each tree-level process with an $\widetilde{\mathcal{O}}_{\mathrm{t}G}$ insertion will therefore be of order $\mathcal{O}(g_s^2 \eta_s)$, which will introduce the sign dependency. Since no double insertion of effective operators will be considered, this logic also extends to all relevant higher order processes. Due to the necessity that any physical result must be independent of the overall choice of this sign, corresponding parameters have to absorb this additional sign, which in this case is the general Wilson coefficient $\widetilde{C}_{\mathrm{t}G}$.

In conclusion, the easiest way to take this sign convention into account is to artificially define the operator $\widetilde{\mathcal{O}}_{\mathrm{t}G}$ with the additional factor η_s

$$\widetilde{\mathcal{O}}_{\mathrm{t}G} \to \widetilde{\mathcal{O}}'_{\mathrm{t}G} = \eta_s \, \widetilde{\mathcal{O}}_{\mathrm{t}G} \,,$$

while substituting the occurring signs in equations 2.26 and 2.27 with a $+1$ (as written in section 1.2.1).

2.4. Setup

To check the validity and correct implementation of the current WHIZARD + GOSAM framework, the approach will be to compare it with already existing results for $t\bar{t}H$ production with SMEFT by Maltoni et al. [18].

For this setup, a UFO model has been created with some modifications as described in section 2.2. In this section, the specific choices regarding parameters and counterterms are discussed, while the paper by Maltoni et al. acts as the main guideline.

The relevant parameters are thereby fixed to the following values

$$\begin{aligned} m_t = 172.5\,\mathrm{GeV}\ ; \quad m_H = 125\,\mathrm{GeV}\ ; \quad m_Z = 91.1876\,\mathrm{GeV} \\ G_f = 1.16637 \cdot 10^{-5}\,\mathrm{GeV}^{-2}\ ; \quad \alpha_{EW} = 7.81861 \cdot 10^{-3}\ , \end{aligned}$$

in accordance with [18]. The renormalization and factorization scale is set accordingly at $\mu_\mathrm{R} = \mu_\mathrm{F} = m_t + m_\mathrm{H}/2$, while the general scale at which the theory is based around is $\mu_{EFT} = m_t$.

The anomalous dimension matrix for the Wilson coefficients can be constructed based on the generalized RGEs in chapter 2.1.3. To reproduce the values in the Maltoni et al. paper, the parameters x_i, a_i and b_i are set to

$$\begin{aligned} a_1 &= -3 & b_1 &= 0 & x_1 &= 1 \\ a_2 &= -2 & b_2 &= 0 & x_2 &= \frac{1}{2} \\ a_3 &= -1 & b_3 &= -1 & x_3 &= -1\ , \end{aligned}$$

which is based on their definitions of the effective operators. The value x_2 is necessary because they introduce the convention of always adding the hermitian conjugate to each operator, even if it is already hermitian (which doubles the contribution of $\mathcal{O}_{\varphi G}$). The value x_3 comes from the discussion in chapter 2.3 on the sign convention choice for η_s. It turns out that one needs to choose $\eta_s^\mathrm{M} = -1$ in order to be consistent with their results. Another essential step is to set the ϑ parameter from section 2.1.3 equal to zero. This is equivalent to the statement that the additional Yukawa couplings y_t in the general effective operators are not renormalized. These are only introduced in order to keep track of the correct QED/Yukawa order in all processes but will not take part in any renormalization procedure. All of these configurations then lead to the anomalous dimension matrix

$$\frac{\mathrm{d}}{\mathrm{d}\ln(\mu)} \begin{pmatrix} \widetilde{C}^\mathrm{M}_{\mathrm{t}\varphi} \\ \widetilde{C}^\mathrm{M}_{\varphi G} \\ \widetilde{C}^\mathrm{M}_{\mathrm{t}G} \end{pmatrix} = \frac{\alpha_s}{\pi} \begin{pmatrix} -2 & 16 & 8 \\ 0 & -7/2 & 1/2 \\ 0 & 0 & 1/3 \end{pmatrix} \begin{pmatrix} \widetilde{C}^\mathrm{M}_{\mathrm{t}\varphi} \\ \widetilde{C}^\mathrm{M}_{\varphi G} \\ \widetilde{C}^\mathrm{M}_{\mathrm{t}G} \end{pmatrix} := \frac{\alpha_s}{\pi}\, \gamma^\mathrm{M} \begin{pmatrix} \widetilde{C}^\mathrm{M}_{\mathrm{t}\varphi} \\ \widetilde{C}^\mathrm{M}_{\varphi G} \\ \widetilde{C}^\mathrm{M}_{\mathrm{t}G} \end{pmatrix}\ , \tag{2.28}$$

which is also in agreement with [18].

Together with the information provided in section 2.1.4, the general counterterms in the DRED scheme can be constructed. In the following, summation over indices is written explicitly for clarity.

First, one finds the relation

$$\frac{\mathrm{d}}{\mathrm{d}\ln(\mu)}\widetilde{C}_i = \sum_j \frac{\alpha_s}{\pi}\gamma_{ij}^{\mathrm{M}}\widetilde{C}_j \overset{2.18}{=} \sum_j \frac{1}{16\pi^2}\left(\delta_{ij}\, b_i\, \frac{\dot{g}_s}{g_s} + \frac{x_i}{x_j}\, y_t^{a_i-a_j} g_s^{b_i-b_j}\,\gamma_{ij}\right)\widetilde{C}_j$$
$$\Rightarrow \quad \gamma_{ij} = \left(-\delta_{ij}\, b_i\, \frac{\dot{g}_s}{g_s} + 16\pi\,\alpha_s\,\gamma_{ij}^{\mathrm{M}}\right)\frac{x_j}{x_i}\, y_t^{a_j-a_i} g_s^{b_j-b_i}\,. \tag{2.29}$$

Then, with equation 2.20

$$\delta^{(-1)} Z_{ij} = \frac{1}{32\pi^2\,\alpha_s}\,\gamma_{ij} \overset{2.29}{=} \left(-\frac{\delta_{ij}\, b_i}{32\pi^2\,\alpha_s}\,\frac{\dot{g}_s}{g_s} + \frac{1}{2\pi}\,\gamma_{ij}^{\mathrm{M}}\right)\frac{x_j}{x_i}\, y_t^{a_j-a_i} g_s^{b_j-b_i}\,. \tag{2.30}$$

The full counterterm in the DRED scheme is then defined as $\delta Z_{ij} = \Delta(\varepsilon)\,\delta^{(-1)} Z_{ij} + \delta^{\mathrm{D}RED} Z_{ij}$, where the DRED shifts can also be taken from section 2.1.4. To transfer these to the general counterterms, equation 2.23 will be used, where from now on only the two operators $\mathcal{O}_{\mathrm{t}\varphi}$ and $\mathcal{O}_{\varphi G}$ will be considered. Here, δZ_y will be set to 0, following the discussion from above for the Yukawa couplings. The total general counterterms then become

$$\delta\widetilde{Z}_{ij} = \delta_{ij}\, b_i \left(\Delta(\varepsilon)\left[-\frac{1}{32\pi^2\,\alpha_s}\,\frac{\dot{g}_s}{g_s} + \delta^{(-1)} Z_g\right] + \delta^{\mathrm{D}RED} Z_g\right)$$
$$+ \Delta(\varepsilon)\,\frac{1}{2\pi}\,\gamma^{\mathrm{M}} + \frac{x_i}{x_j}\, y_t^{a_i-a_j} g_s^{b_i-b_j}\,\delta_{ij}^{\mathrm{D}RED} Z_{ij}\,. \tag{2.31}$$

The occurring ($\overline{\mathrm{MS}}$) counterterm for the strong coupling can be obtained by calculating the 1-loop QCD corrections to a relevant vertex like the ghost-gluon vertex, while using the differing dimensions approach as with the Wilson coefficient counterterms. However, since $\mathcal{O}_{\mathrm{t}G}$ contributions will not be included, one does not need the strong coupling renormalization since the first line on the right-hand side in equation 2.31 is $\sim b_i$, where $b_i = 0$ for $i \in \{\mathrm{t}\varphi, \varphi G\}$. Inserting everything yields the following full counterterm for the Wilson coefficients in the convention from above

$$\delta\widetilde{Z}_{ij}^{\mathrm{M}} = \frac{\Delta(\varepsilon)}{2\pi}\begin{pmatrix} -2 & 16 \\ 0 & -7/2 \end{pmatrix} + \frac{1}{2\pi}\begin{pmatrix} -2/3 & 16/3 \\ 0 & 1/2 \end{pmatrix}\,, \tag{2.32}$$

where $\widetilde{Z}_{ij} = (1 + \alpha_s\,\delta\widetilde{Z}_{ij})$. These are therefore inserted into the corresponding section of the UFO model.

A representative version of the WHIZARD runcard used in this case is shown in appendix A.1. The full setup used in this Thesis, including the UFO model, is available on the GitHub project repository at `https://git.particle.kit.edu/gudrun/tth_smeft/-/tree/main/MasterThesis?ref_type=heads`.

3. Results

The total cross section for the used model may be written in the following form

$$\begin{aligned}\sigma &= \mathcal{M}_{SM\times SM} + \mathcal{M}_{SM\times dim\text{-}6} + \mathcal{M}_{dim\text{-}6\times dim\text{-}6} \\ &= \sigma_{SM} + \sum_i \frac{\widetilde{C}_i^{\mathrm{M}}}{\Lambda^2}\,\sigma_i + \sum_{\substack{i,j \\ i\leq j}} \frac{\widetilde{C}_i^{\mathrm{M}}\,\widetilde{C}_j^{\mathrm{M}}}{\Lambda^4}\,\sigma_{ij}\ ,\end{aligned} \tag{3.1}$$

where the $\mathcal{M}$ are the symbolic contributions from the different diagram domains to the total cross sections. The σ_i and σ_{ij} objects then parameterize these different contributions further into individual terms.

To obtain these results, the Wilson coefficients $\widetilde{C}_i^{\,\mathrm{M}}$ are set to δ_{ij} in the simulation, depending on the desired σ_j. To receive better Monte Carlo error estimations, a special truncation option has been included into GoSam to only generate the corresponding matrix elements for one of the summands from equation 3.1, which can then be numerically evaluated individually by Whizard. The new physics scale is set to $\Lambda = 1\,\mathrm{TeV}$. For the simulation, parton-distributions are needed for which LHAPDF sets are used [45]. All results in leading order are obtained with the MMHT2014lo68cl PDF set, while all next-to-leading order results (including the leading order contributions herein) are evaluated with the MMHT2014nlo68cl PDF set [46]. For the Monte Carlo integration, Whizard is set to 15 iterations with 10^4 calls, except for the real corrections which are performed with $5\cdot 10^4$ calls per iteration. The invariant mass is then set to $\sqrt{s} = 13\,\mathrm{TeV}$, for which the results are shown in tables 3.1 and 3.2. The errors quoted here are the Monte Carlo errors of the Whizard simulation.

The reference values are presented without error values, since the Monte Carlo error of these numbers are not known.

The NLO results of Whizard are given individually as the different contributions of the total cross section: LO (Leading Order / Born), R (Real Emission), V (Virtual Correction) and D (DGLAP / PDF Evolution). The total cross section can be split up into these different domains

$$\sigma^{NLO} = \sigma^{LO} + \underbrace{\int_{n+1}\left(\mathrm{d}\sigma^{\mathrm{R}'} - \mathrm{d}\sigma^{\mathrm{S}}\right)}_{:=\sigma^{\mathrm{R}}} + \underbrace{\int_n \left(\mathrm{d}\sigma^{\mathrm{V}'} + \int_{rad}\mathrm{d}\sigma^{S}\right)}_{:=\sigma^{\mathrm{V}}} + \sigma^{\mathrm{D}GLAP}\ ,$$

where Whizard uses the FKS subtraction [47] to construct the IR subtraction term σ^{S}. The σ^{R} and σ^{V} contributions are then individually finite so that they can be evaluated numerically. The DGLAP term considers the evolution of the parton density functions as a function of the energy scale [48–50].

Table 3.1.: LO results for the cross section contributions at $\sqrt{s} = 13\,\mathrm{TeV}$ obtained with WHIZARD and the reference values from [18].

	σ_{SM} / [fb]	$\sigma_{t\varphi}$ / [fb]	$\sigma_{\varphi G}$ / [fb]
WHIZARD total	463.49 ± 0.73	-55.17 ± 0.08	626.01 ± 1.10
Reference	464	-55	627

	$\sigma_{t\varphi,t\varphi}$ / [fb]	$\sigma_{\varphi G,\varphi G}$ / [fb]	$\sigma_{t\varphi,\varphi G}$ / [fb]
WHIZARD total	1.642 ± 0.002	646.21 ± 1.04	-37.79 ± 1.44
Reference	1.6	646	-37

Table 3.2.: NLO results for the cross section contributions at $\sqrt{s} = 13\,\mathrm{TeV}$ obtained with WHIZARD and the reference values from [18].

	σ_{SM} / [fb]	$\sigma_{t\varphi}$ / [fb]	$\sigma_{\varphi G}$ / [fb]
WHIZARD LO	403.14 ± 0.63	-47.98 ± 0.08	542.42 ± 0.95
WHIZARD R	6.94 ± 0.25	$-\ 0.84 \pm 0.03$	50.34 ± 0.38
WHIZARD V	24.60 ± 0.06	$-\ 5.06 \pm 0.01$	182.58 ± 0.42
WHIZARD D	70.72 ± 0.32	$-\ 8.42 \pm 0.04$	94.33 ± 0.48
WHIZARD total	505.40 ± 0.75	-62.30 ± 0.09	869.67 ± 1.21
Reference	507	-62	872

	$\sigma_{t\varphi,t\varphi}$ / [fb]	$\sigma_{\varphi G,\varphi G}$ / [fb]	$\sigma_{t\varphi,\varphi G}$ / [fb]
WHIZARD LO	1.428 ± 0.002	549.45 ± 0.87	-32.72 ± 2.54
WHIZARD R	0.024 ± 0.001	63.27 ± 0.46	$-\ 2.96 \pm 1.10$
WHIZARD V	0.214 ± 0.000	386.55 ± 0.67	-12.46 ± 0.95
WHIZARD D	0.250 ± 0.001	19.64 ± 0.60	$-\ 5.64 \pm 1.38$
WHIZARD total	1.917 ± 0.003	1018.91 ± 1.33	-53.78 ± 3.23
Reference	1.9	1021	-53

The error given in the case of $\sigma_{\mathrm{t}\varphi,\varphi G}$ is a naive estimation, since it is always produced alongside of $\sigma_{\mathrm{t}\varphi,t\varphi}$ and $\sigma_{\varphi G,\varphi G}$. Its value is retrieved via

$$\sigma_{\mathrm{t}\varphi,\varphi G} = \mathcal{M}_{\mathrm{dim\text{-}6}\times dim\text{-}6} - \sigma_{\mathrm{t}\varphi,t\varphi} - \sigma_{\varphi G,\varphi G} \ ,$$

where the error is then obtained with simple error propagation in the same way. This is not completely correct, since the errors of all σ_{ij} are generally correlated. However, in this setting it is not possible to consider this correlation in a clean way, which is why the approach from above is used as a rough estimation.

As can be seen, all results from the WHIZARD + GOSAM framework provide a good match with the reference values. At LO, the largest relative deviation can be observed for the $\mathrm{t}\varphi, \mathrm{t}\varphi$ contribution at around $2,56\,\%$. At NLO, the $\mathrm{t}\varphi, \varphi\mathrm{G}$ contribution has the leading difference to its reference with $1,47\,\%$. However, especially when taking the Monte Carlo errors into account, these deviations are well withing the range of acceptability. As the reference values do not come with a comparable error, one can at least assume some general rounding errors at half of the last given digit, which then brings almost all values into agreement within the range of uncertainty.

With these results, the value of the cross section can be probed theoretically by using equation 3.1. The value obtained with this equation will be called the *total* cross section. When only the order $\mathcal{O}(\Lambda^{-2})$ suffices, even on cross section level, one can truncate the term quadratic in the Wilson coefficients to obtain the *linear* cross section

$$\sigma_{linear} := \mathcal{M}_{\mathrm{SM}\times SM} \ + \ \mathcal{M}_{\mathrm{SM}\times dim\text{-}6} = \sigma_{\mathrm{SM}} + \sum_i \frac{\widetilde{C}_i^{\mathrm{M}}}{\Lambda^2}\,\sigma_i \ .$$

Both are shown at NLO normalized to the SM cross section as a function of the Wilson coefficients in figure 3.1 and 3.2. The scale of each Wilson coefficient is chosen such that it roughly respects the current constraints on the coefficients [20].

One can see that in both cases $\widetilde{C}^{\mathrm{M}}_{\varphi\mathrm{G}}$ contributes more significantly to the presented ratio of the cross sections than $\widetilde{C}^{\mathrm{M}}_{\mathrm{t}\varphi}$, which of course reflects the result $|\sigma_{\varphi\mathrm{G}}| > |\sigma_{\mathrm{t}\varphi}|$. In the plot of the total cross section, an almost symmetric behavior can be seen (more prominently along the $\varphi\mathrm{G}$ axis), stemming from the fact that the shape of the function is dictated by its quadratic structure in the Wilson coefficients. The linear cross section shows regions that become negative. Since these values are regarded as (a ratio of) probabilities, this region is clearly unphysical. However, both approaches offer valid interpretations. The total cross section includes all contributions up to $\mathcal{O}(\Lambda^{-2})$ on amplitude level, whereas the linear cross section only allows terms up to $\mathcal{O}(\Lambda^{-2})$ on cross section level. So it is the decision of which domain to expand in that determines this specific truncation.

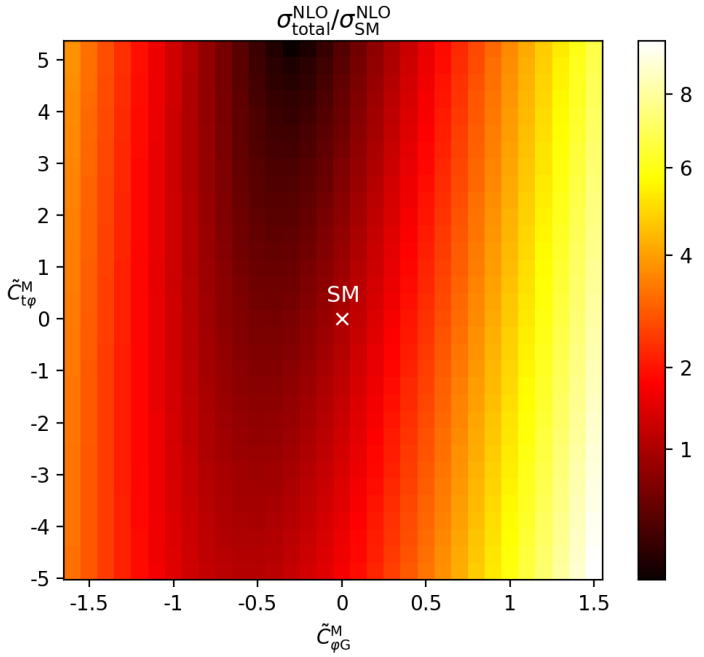

Figure 3.1.: The full cross section at NLO normalized to the SM cross section for different values of the Wilson coefficients.

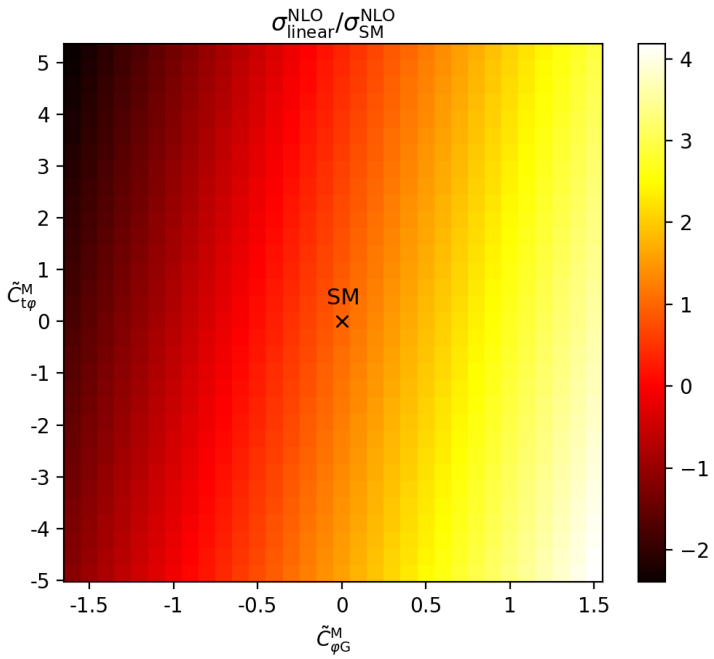

Figure 3.2.: The cross section up to linear order of the Wilson coefficients at NLO normalized to the SM cross section.

4. Conclusion

The desired implementation of this custom SMEFT model has succeeded, as the results and their validation show. It should be noted, however, that this is not a straight-forward path since many manual adjustments are necessary. The main difficulty on the theory side consists of renormalization. The current setup and functionality of the Whizard + GoSam framework requires a manual specification of counterterms, which have to be defined for each case individually due to the mixing of the effective operators. Further complications arise because of the deviation from the conventional Warsaw basis. This necessitates a generalized approach to the RGEs and counterterms of the Wilson coefficients.

In addition to the theoretical discussion, there are also a number of technical aspects to consider. The internal structure of GoSam and its interaction with the UFO format fixes certain freedoms that must be respected when constructing the theory. This makes the adoption of a certain remormalization scheme or a certain sign convention almost inevitable. Before the changes were made, GoSam also made a number of additional assumptions that would not be compatible with the desired implementation of this SMEFT approach and had to be fixed accordingly. Similarly, the UFO model output from the SmeftFR package is not suitable for direct use in this project. In particular, the ambivalent couplings, the complex-valued parameters, and the large number of redundant definitions interfere with the process and slow it down significantly. In addition, further technical optimizations were added, such as the truncation of the SMEFT orders for a more precise evaluation of the individual results.

Many of the adjustments that were made were the result of trial and error, as it was not clear from the outset what was already taken into account by the framework during implementation, nor that there were still hidden problems that would lead to incorrect calculations. This took a lot of time, which is why a structured and organized way of working should definitely be called for in future implementations, as well as a more detailed preparation and documentation of GoSam.

In conclusion, the desired implementation has been successful, and the documented work presented in this thesis offers a basic foundation to expand upon in order to implement similar SMEFT or general EFT approaches for Whizard + GoSam in the future. Automating some procedures, in particular the renormalization, would save a lot of time, especially if this framework is to be used in various physics applications, but is certainly anything but trivial. However, this thesis also shows that this setup has the potential to become a general tool for SMEFT calculations and should encourage further development and use.

Bibliography

[1] F. Englert and R. Brout. "Broken Symmetry and the Mass of Gauge Vector Mesons". In: *Phys. Rev. Lett.* 13 (1964). Ed. by J. C. Taylor, pp. 321–323. DOI: 10.1103/PhysRevLett.13.321.

[2] Peter W. Higgs. "Broken symmetries, massless particles and gauge fields". In: *Phys. Lett.* 12 (1964), pp. 132–133. DOI: 10.1016/0031-9163(64)91136-9.

[3] Peter W. Higgs. "Broken Symmetries and the Masses of Gauge Bosons". In: *Phys. Rev. Lett.* 13 (1964). Ed. by J. C. Taylor, pp. 508–509. DOI: 10.1103/PhysRevLett.13.508.

[4] G. S. Guralnik, C. R. Hagen, and T. W. B. Kibble. "Global Conservation Laws and Massless Particles". In: *Phys. Rev. Lett.* 13 (1964). Ed. by J. C. Taylor, pp. 585–587. DOI: 10.1103/PhysRevLett.13.585.

[5] Peter W. Higgs. "Spontaneous Symmetry Breakdown without Massless Bosons". In: *Phys. Rev.* 145 (4 May 1966), pp. 1156–1163. DOI: 10.1103/PhysRev.145.1156. URL: https://link.aps.org/doi/10.1103/PhysRev.145.1156.

[6] T. W. B. Kibble. "Symmetry Breaking in Non-Abelian Gauge Theories". In: *Phys. Rev.* 155 (5 Mar. 1967), pp. 1554–1561. DOI: 10.1103/PhysRev.155.1554. URL: https://link.aps.org/doi/10.1103/PhysRev.155.1554.

[7] Georges Aad et al. "Observation of a new particle in the search for the Standard Model Higgs boson with the ATLAS detector at the LHC". In: *Phys. Lett. B* 716 (2012), pp. 1–29. DOI: 10.1016/j.physletb.2012.08.020. arXiv: 1207.7214 [hep-ex].

[8] Serguei Chatrchyan et al. "Observation of a New Boson at a Mass of 125 GeV with the CMS Experiment at the LHC". In: *Phys. Lett. B* 716 (2012), pp. 30–61. DOI: 10.1016/j.physletb.2012.08.021. arXiv: 1207.7235 [hep-ex].

[9] Albert M Sirunyan et al. "Observation of $t\bar{t}H$ production". In: *Phys. Rev. Lett.* 120.23 (2018), p. 231801. DOI: 10.1103/PhysRevLett.120.231801. arXiv: 1804.02610 [hep-ex].

[10] M. Aaboud et al. "Observation of Higgs boson production in association with a top quark pair at the LHC with the ATLAS detector". In: *Phys. Lett. B* 784 (2018), pp. 173–191. DOI: 10.1016/j.physletb.2018.07.035. arXiv: 1806.00425 [hep-ex].

[11] Howard E. Haber and Laurel Stephenson Haskins. "Supersymmetric theory and models." In: *Theoretical Advanced Study Institute in Elementary Particle Physics: Anticipating the Next Discoveries in Particle Physics*. WSP, 2018, pp. 355–499. DOI: 10.1142/9789813233348_0006. arXiv: 1712.05926 [hep-ph].

[12] Igor Garcia Irastorza. "An introduction to axions and their detection". In: *SciPost Phys. Lect. Notes* 45 (2022), p. 1. DOI: 10.21468/SciPostPhysLectNotes.45. arXiv: 2109.07376 [hep-ph].

[13] Scott Willenbrock and Cen Zhang. "Effective Field Theory Beyond the Standard Model". In: *Ann. Rev. Nucl. Part. Sci.* 64 (2014), pp. 83–100. DOI: 10.1146/annurev-nucl-102313-025623. arXiv: 1401.0470 [hep-ph].

[14] Riccardo Penco. "An Introduction to Effective Field Theories". In: (June 2020). arXiv: 2006.16285 [hep-th].

[15] D. Azevedo et al. "CP tests of Higgs couplings in $t\bar{t}h$ semileptonic events at the LHC". In: *Phys. Rev. D* 98.3 (2018), p. 033004. DOI: 10.1103/PhysRevD.98.033004. arXiv: 1711.05292 [hep-ph].

[16] Rahool Kumar Barman, Dorival Gonçalves, and Felix Kling. "Machine learning the Higgs boson-top quark CP phase". In: *Phys. Rev. D* 105.3 (2022), p. 035023. DOI: 10.1103/PhysRevD.105.035023. arXiv: 2110.07635 [hep-ph].

[17] Matthew R. Buckley and Dorival Goncalves. "Boosting the Direct CP Measurement of the Higgs-Top Coupling". In: *Phys. Rev. Lett.* 116.9 (2016), p. 091801. DOI: 10.1103/PhysRevLett.116.091801. arXiv: 1507.07926 [hep-ph].

[18] Fabio Maltoni, Eleni Vryonidou, and Cen Zhang. "Higgs production in association with a top-antitop pair in the Standard Model Effective Field Theory at NLO in QCD". In: *Journal of High Energy Physics* 2016.10 (Oct. 2016). ISSN: 1029-8479. DOI: 10.1007/jhep10(2016)123. URL: http://dx.doi.org/10.1007/JHEP10(2016)123.

[19] Dario Buttazzo et al. "Investigating the near-criticality of the Higgs boson". In: *JHEP* 12 (2013), p. 089. DOI: 10.1007/JHEP12(2013)089. arXiv: 1307.3536 [hep-ph].

[20] Eugenia Celada et al. "Mapping the SMEFT at high-energy colliders: from LEP and the (HL-)LHC to the FCC-ee". In: *JHEP* 09 (2024), p. 091. DOI: 10.1007/JHEP09(2024)091. arXiv: 2404.12809 [hep-ph].

[21] Wikipedia. *Standard Model — Wikipedia, The Free Encyclopedia*. http://en.wikipedia.org/w/index.php?title=Standard%20Model&oldid=1252767306. [Online; accessed 27-October-2024]. 2024.

[22] JORGE C. ROMÃO and JOÃO P. SILVA. "A RESOURCE FOR SIGNS AND FEYNMAN DIAGRAMS OF THE STANDARD MODEL". In: *International Journal of Modern Physics A* 27.26 (Oct. 2012), p. 1230025. ISSN: 1793-656X. DOI: 10.1142/s0217751x12300256. URL: http://dx.doi.org/10.1142/S0217751X12300256.

[23] R. V. Harlander, S. Y. Klein, and M. Lipp. "FeynGame". In: *Comput. Phys. Commun.* 256 (2020), p. 107465. DOI: 10.1016/j.cpc.2020.107465. arXiv: 2003.00896 [physics.ed-ph].

[24] B. Grzadkowski et al. "Dimension-Six Terms in the Standard Model Lagrangian". In: *JHEP* 10 (2010), p. 085. DOI: 10.1007/JHEP10(2010)085. arXiv: 1008.4884 [hep-ph].

[25] Wolfgang Kilian, Thorsten Ohl, and Jurgen Reuter. "WHIZARD: Simulating Multi-Particle Processes at LHC and ILC". In: *Eur. Phys. J. C* 71 (2011), p. 1742. DOI: 10.1140/epjc/s10052-011-1742-y. arXiv: 0708.4233 [hep-ph].

[26] Gavin Cullen et al. "G$OSAM$-2.0: a tool for automated one-loop calculations within the Standard Model and beyond". In: *Eur. Phys. J. C* 74.8 (2014), p. 3001. DOI: 10.1140/epjc/s10052-014-3001-5. arXiv: 1404.7096 [hep-ph].

[27] T. Binoth et al. "A Proposal for a Standard Interface between Monte Carlo Tools and One-Loop Programs". In: *Comput. Phys. Commun.* 181 (2010). Ed. by Genevieve Belanger, Fawzi Boudjema, and Jean-Philippe Guillet, pp. 1612–1622. DOI: 10.1016/j.cpc.2010.05.016. arXiv: 1001.1307 [hep-ph].

[28] Paulo Nogueira. "Automatic Feynman Graph Generation". In: *J. Comput. Phys.* 105 (1993), pp. 279–289. DOI: 10.1006/jcph.1993.1074.

[29] J. A. M. Vermaseren. "New features of FORM". In: (Oct. 2000). arXiv: math-ph/0010025.

[30] J. Kuipers et al. "FORM version 4.0". In: *Comput. Phys. Commun.* 184 (2013), pp. 1453–1467. DOI: 10.1016/j.cpc.2012.12.028. arXiv: 1203.6543 [cs.SC].

[31] P. Mastrolia et al. "Scattering AMplitudes from Unitarity-based Reduction Algorithm at the Integrand-level". In: *JHEP* 08 (2010), p. 080. DOI: 10.1007/JHEP08(2010)080. arXiv: 1006.0710 [hep-ph].

[32] G. Cullen et al. "Golem95C: A library for one-loop integrals with complex masses". In: *Comput. Phys. Commun.* 182 (2011), pp. 2276–2284. DOI: 10.1016/j.cpc.2011.05.015. arXiv: 1101.5595 [hep-ph].

[33] Tiziano Peraro. "Ninja: Automated Integrand Reduction via Laurent Expansion for One-Loop Amplitudes". In: *Comput. Phys. Commun.* 185 (2014), pp. 2771–2797. DOI: 10.1016/j.cpc.2014.06.017. arXiv: 1403.1229 [hep-ph].

[34] A. van Hameren. "OneLOop: For the evaluation of one-loop scalar functions". In: *Comput. Phys. Commun.* 182 (2011), pp. 2427–2438. DOI: 10.1016/j.cpc.2011.06.011. arXiv: 1007.4716 [hep-ph].

[35] R. Keith Ellis and Giulia Zanderighi. "Scalar one-loop integrals for QCD". In: *JHEP* 02 (2008), p. 002. DOI: 10.1088/1126-6708/2008/02/002. arXiv: 0712.1851 [hep-ph].

[36] Thorsten Ohl. "Vegas revisited: Adaptive Monte Carlo integration beyond factorization". In: *Comput. Phys. Commun.* 120 (1999), pp. 13–19. DOI: 10.1016/S0010-4655(99)00209-X. arXiv: hep-ph/9806432.

[37] Matthias Neubert. *Les Houches Lectures on Renormalization Theory and Effective Field Theories*. 2020. arXiv: 1901.06573 [hep-ph].

[38] Elizabeth E. Jenkins, Aneesh V. Manohar, and Michael Trott. "Renormalization group evolution of the standard model dimension six operators. I: formalism and dependence". In: *Journal of High Energy Physics* 2013.10 (Oct. 2013). ISSN: 1029-8479. DOI: 10.1007/jhep10(2013)087. URL: http://dx.doi.org/10.1007/JHEP10(2013)087.

[39] Elizabeth E. Jenkins, Aneesh V. Manohar, and Michael Trott. "Renormalization group evolution of the Standard Model dimension six operators II: Yukawa dependence". In: *Journal of High Energy Physics* 2014.1 (Jan. 2014). ISSN: 1029-8479. DOI: 10.1007/jhep01(2014)035. URL: http://dx.doi.org/10.1007/JHEP01(2014)035.

[40] Rodrigo Alonso et al. "Renormalization group evolution of the Standard Model dimension six operators III: gauge coupling dependence and phenomenology". In: *Journal of High Energy Physics* 2014.4 (Apr. 2014). ISSN: 1029-8479. DOI: 10.1007/jhep04(2014)159. URL: http://dx.doi.org/10.1007/JHEP04(2014)159.

[41] Celine Degrande et al. "UFO - The Universal FeynRules Output". In: *Comput. Phys. Commun.* 183 (2012), pp. 1201–1214. DOI: 10.1016/j.cpc.2012.01.022. arXiv: 1108.2040 [hep-ph].

[42] Luc Darmé et al. "UFO 2.0: the 'Universal Feynman Output' format". In: *Eur. Phys. J. C* 83.7 (2023), p. 631. DOI: 10.1140/epjc/s10052-023-11780-9. arXiv: 2304.09883 [hep-ph].

[43] Adam Alloul et al. "FeynRules 2.0— A complete toolbox for tree-level phenomenology". In: *Computer Physics Communications* 185.8 (Aug. 2014), pp. 2250–2300. ISSN: 0010-4655. DOI: 10.1016/j.cpc.2014.04.012. URL: http://dx.doi.org/10.1016/j.cpc.2014.04.012.

[44] A. Dedes et al. "SmeftFR v3 – Feynman rules generator for the Standard Model Effective Field Theory". In: *Computer Physics Communications* 294 (Jan. 2024), p. 108943. ISSN: 0010-4655. DOI: 10.1016/j.cpc.2023.108943. URL: http://dx.doi.org/10.1016/j.cpc.2023.108943.

[45] Andy Buckley et al. "LHAPDF6: parton density access in the LHC precision era". In: *Eur. Phys. J. C* 75 (2015), p. 132. DOI: 10.1140/epjc/s10052-015-3318-8. arXiv: 1412.7420 [hep-ph].

[46] L. A. Harland-Lang et al. "Parton distributions in the LHC era: MMHT 2014 PDFs". In: *Eur. Phys. J. C* 75.5 (2015), p. 204. DOI: 10.1140/epjc/s10052-015-3397-6. arXiv: 1412.3989 [hep-ph].

[47] S. Frixione, Z. Kunszt, and A. Signer. "Three jet cross-sections to next-to-leading order". In: *Nucl. Phys. B* 467 (1996), pp. 399–442. DOI: 10.1016/0550-3213(96)00110-1. arXiv: hep-ph/9512328.

[48] V. N. Gribov and L. N. Lipatov. "Deep inelastic e p scattering in perturbation theory". In: *Sov. J. Nucl. Phys.* 15 (1972), pp. 438–450.

[49] Yuri L. Dokshitzer. "Calculation of the Structure Functions for Deep Inelastic Scattering and e+ e- Annihilation by Perturbation Theory in Quantum Chromodynamics." In: *Sov. Phys. JETP* 46 (1977), pp. 641–653.

[50] Guido Altarelli and G. Parisi. "Asymptotic Freedom in Parton Language". In: *Nucl. Phys. B* 126 (1977), pp. 298–318. DOI: 10.1016/0550-3213(77)90384-4.

A. Appendix

A.1. WHIZARD Runcard

The runcard used with WHIZARD in this thesis has the structure that is presented in the following. It has the setup to represent a run to calculate the full cross section for the SM at NLO as an example.

First, the header declares the UFO model that one wants to use

```
model = SMEFT_tphi_phiG_UFO (ufo ("/path/to/ufo/directory"))
```

After which the main masses, scales and Wilson coefficients are set, which either corresponds to their definitions in the UFO files or in GOSAM directly

```
######################
# physics parameters #
######################
MQB = 0
MLT = 0
MQT = 172.5 GeV
WQT = 0 GeV
Hmass = 125.0 GeV

Gf = 0.0000116637
Zmass = 91.1876
aS = 0.1184

fmu3x3 = MQT
mueft = MQT

Cuphi3x3 = 0
CphiG = 0
```

The Wilson coefficients can be set to 1. (or any other value) here to produce the EFT results. After this, the process itself is defined by setting the invariant mass, the necessary scales and PDFs but also additional filters and options for GOSAM to use optimizations during the matrix element generation. The filter options remove all couplings between the Higgs boson (part25) and any light quarks (part1, …, part5).

```
#################
# process setup #
#################
sqrts = 13000 GeV

renormalization_scale = 1.*(MQT+MH/2.0)
factorization_scale = 1.*(MQT+MH/2.0)

beams = p, p => lhapdf
$lhapdf_file = "MMHT2014nlo68cl"

?alphas_is_fixed = false
?alphas_from_lhapdf = true
alpha_power = 1
alphas_power = 2

$nlo_correction_type = "QCD"

$method = "gosam"

$gosam_filter_lo = "lambda d: d.vertices(part25,part1,anti1)==0
and ... and d.vertices(part25,part5,anti5)==0 and d.order('NP')<2"
$gosam_filter_nlo = "lambda d: d.vertices(part25,part1,anti1)==0
and ... and d.vertices(part25,part5,anti5)==0 and d.order('NP')<2"
$gosam_extra_cmd = "all_mandelstam=True
order_names=QCD,NP
enable_truncation_orders=True
flavour_groups=1:2:3:4:5
respect_generations=True
use_vertex_labels=True
renorm_eftwilson=True
finite_renorm_ehc=False
filter.ct=lambda d: d.vertices(part25,part1,anti1)==0
and ... and d.vertices(part25,part5,anti5)==0 and d.order('NP')<2"
gosam_eftcount=0

alias U = "u~"
alias D = "d~"
alias S = "s~"
alias C = "c~"
alias B = "b~"
alias T = "t~"
alias gl = "g"

alias pr = gl:u:U:d:D:c:C:s:S:b:B

$exclude_gauge_splittings = "t"

process pp_ttH_lo = pr, pr => t, T, H { nlo_calculation = full }

$compile_workspace = "libs_lo"

compile ()
```

The final part is concerned with the Monte Carlo integration to obtain the final cross section. Here, precision and the integration procedure can be finetuned further. The seed is set automatically but will be chosen to be 1 for clarity

```
###############
# integration #
###############
relative_error_goal = 0.001

$integrate_workspace = "grid_lo"

?vis_history = true

seed = 1
integrate(pp_ttH_lo) { iterations = 15:10000:"gw" }
```

All results in this thesis can be reproduced by this runcard and the corresponding UFO model by varying the Wilson coefficients accordingly. The full project files can be found at `https://git.particle.kit.edu/gudrun/tth_smeft/-/tree/main/MasterThesis?ref_type=heads`.